



**Politecnico
di Torino**

Politecnico di Torino

Architettura Costruzione Città

2020/2021

Sessione di Laurea Dicembre 2021

**AMBISONICS AS A TOOL FOR ARCHITECTURAL
PRESERVATION. THE VIRTUAL SOUNDSCAPE
OF THE ANCIENT THEATRE OF TINDARI**

Relatori:

Arianna Astolfi

Correlatori:

Louena Shtrepi

Angelo Farina

Candidati:

Lorenzo Lavagna

ABSTRACT

The acoustic environment is very influential on how we experience some of our architectural heritage. This is especially relevant for ancient amphitheaters, that were designed to achieve high sound quality and good speech intelligibility, and this is why they are one of the main themes of the emerging field of archeoacoustics.

It is important to properly measure, document, and make virtual reconstructions of the acoustics of these places in order to preserve and communicate their behavior, opening the possibility to experience spaces that are no more accessible.

The object of this investigation is the soundscape of the theatre of Tindari, which has changed considerably during the centuries. A combination of visual and acoustic experience in a virtual reality environment can provide an immersive exploration of all the phases of its evolution, aiming to be helpful for researchers and to attract more focused attention from a broader public.

The visual rendering consists of equirectangular panoramic images, reconstructed from several viewing points, each associated with an High Order Ambisonics impulse response, computed with the hybrid ray tracing and image source method of Odeon, and the pyramid tracing algorithm of Ramsete. Anechoic samples are then convolved with these impulse responses to create the virtual soundtrack for each viewing point. The results are stored in video files with proper metadata, which allow them to be watched with an HMD (such as an Oculus Quest 2) or to be uploaded on Youtube.

The study makes use of the results of a previous research, which has validated an accurate acoustic model of the current deteriorated state of the theater by matching the acoustic parameters obtained in the virtual simulation with those obtained by real on-site measurements. From this baseline, the shapes and materials of the virtual model can be modified to represent the previous configurations of the theatre and listen to how they sounded.

This study further develops the analysis of the acoustics of the theatre, compares different methods of acoustic reconstruction in order to test their accuracy and their limits, and finally presents the results of the virtual reconstruction of the theatre in its current state, in two of its previous configurations and one proposed future configuration.

SUMMARY

1. INTRODUCTION.....	6
1.1 Archeoacoustics and sensory history.....	6
1.2 Architecture and Ambisonics.....	7
1.3 Previous works on the theatre of Tindari.....	8
2. AMBISONICS.....	9
2.1 Spherical harmonics.....	10
3. ARCHEOACOUSTICS: LITERARY REVIEW	13
3.1 Studies on the on ancient theatres	13
3.3 The ISO 3382-1:2009	16
4. Framework of the case study.....	19
4.1 Territorial framework	19
4.3 Historical framework.....	21
4.4 Current conditions of the theatre.....	21
5. PREVIOUS WORKS ON THE THEATRE OF TINDARI	25
5.1 The measurement campaign of 2015.....	25
5.3 The simulation of the current state.....	26
5.4 Reconstruction of the historical phases	32
6. METHODOLOGY AND RESULTS.....	36
6.1 Comparing Odeon and Ramsete.....	36
6.2 The creation of the new model	39
6.3 Results of the calibration	45
6.4 Reconstruction of the past	48
6.5 Proposed future configuration	55
6.6 Comparison between the configurations.....	59

7. AURALIZATION AND VIRTUAL REALITY	60
7.1 Auralization	60
7.2 The visual component	60
7.3 The audio component	61
7.4 La creazione dei video in VR	62
8. CONCLUSIONS	67
9. REFERENCES	68
LIST OF FIGURES	72
LIST OF TABLES	74

1. INTRODUCTION

1.1 Archeoacoustics and sensory history

Recent year have seen an increasing number of interdisciplinary approaches aimed towards an holistic methodology to the investigatory historic remains, and to the overcoming of ocular-centric models of inquiry and transmission of knowledge.

Archeoacoustic is one of these approaches, merging the contributions and practices of acoustics, archaeology, computer simulation, cultural anthropology, musicology and architecture.

The research on the connection of architecture and sound dates back to the I century BC, when Vitruvius dedicated an entire chapter of his *De Architectura* to the laws of harmony. Nowadays the technological advancement in the acoustic field are seen as a new opportunity to develop a deeper knowledge on that consistent portion of our architectural heritage whose character is deeply connected to the acoustic experience that it offers, and also as tool to communicate its importance and promote their preservation.

This thesis was inspired by an ongoing European project, part of the JPI CH (Joint Programming Initiatives on Cultural Heritage) called *The Past Has Ears*.

1.1.1 The Past Has Ears (PHE)

The acronym of this European project (Phé, for the constellation Phoenix) is a perfect synthesis of the reasons behind its ideation and its objectives. It was in fact inspired by the relatively recent fires at *Cathédrale de Notre Dame de Paris* and *Teatro La Fenice* opera hall and it focuses on bringing them back from the ashes by reconstructing them in virtual reality (Katz, Murphy and Farina, 2020).

The three main objectives identified for this research project are:

1. Documentation: developing a framework protocol for digital documentation through precise measurements of the acoustic state of a site that is sufficient for providing a safeguarded reference in the event of evolutions of the site, or in the event of disaster to the site.

Creating an open public database providing much needed data on acoustic and physical properties of materials rarely used in modern constructions, and therefore poorly documented.

2. Modelling: making use of the latest digital reconstruction methods and the recent evolutions in computational technologies to achieve an improved quality and resolution of acoustic modelling.
3. Presentation: integrating the workflows of multiple disciplines such as acoustic research, musicology and 3d production to create a person-scale immersive experience, focusing on the observation position to convey information through both the sense of sight and hearing.

Three heritage sites are participating as case studies: Tindari Theatre (IT), Notre-Dame de Paris Cathedral (FR), and The Houses of Parliament (UK). Concerning the case study of the Theatre of Tindari, the plan of this project is to: “to first measure the acoustical properties of the theater in its current configuration, and use these data for carefully tuning the Ramsete room acoustics and auralization software, so that the numerical simulations are in close agreement with reality.

Then it is planned to reconstruct acoustics during Greek times, during Roman times, during the Middle Ages, and after its renovation in the 20th century. It will be possible to listen to the different acoustical soundscapes both using a full audio-visual Virtual Reality system, and onsite, using binaural headtracked headphones (augmented reality).“(‘The Past Has Hears (PHE) JPICH Conservation and Protection Call Application’, 2020)

1.2 Architecture and Ambisonics

The idea of documenting the sound field of the building of our architectural heritage is as old as spatial audio itself. It was first proposed by Michael Anthony Gerzon, in the 70s in his famous article ‘Recording concert hall acoustics for posterity’, (Gerzon, 1975).

During the 1970s Michael Gerzon, led by his passion for musical performances, and wanting to achieve a faithful documentation and reproduction of the immersive experience of a concert hall, invented, with the participation of Peter Craven, what we now call Ambisonics, a 3D audio surround rendering and representation approach first developed.

It is widely recognized that the space surrounding a performance plays an essential role on the listening experience, many composers focused on this relationship, especially during the 20th century, i.e. Stockhausen, Boulez and Xenakis. (Cole, 2007)

The relationship also works the other way around: as space impacts the experience of sound, sound impacts the experience of space.

However sometimes this correlation is underrated by architects.

Quoting the article "Dear Architects: Sound Matters" written by Michael Kimmelman for the New York Times:

"Sound is really important," Ricardo Scofidio, from Diller Scofidio & Renfro, who helped design the High Line, acknowledged. But then he said, unless you're an architect designing a concert hall, "you're not thinking about how you might produce a specific sound." He added, "That's partly because the process of making models and drawings doesn't allow for it." Besides, clients don't ask much about what a house will sound like. (Kimmelman, 2015)

This also because the tools to design the soundscape of a building are often not accessible to architects.

The objective of this theses is to propose the method of Ambisonics as a tool to better understand our experience of space, and as a guide to imagine new possibilities for or architectural heritage.

The thesis will describe the process of creating an accurate acoustic simulation of the case study in both its current state, in two of its previous configurations, and in one proposed state of project (in Chapter 6).

The last Chapter will show how the outputs of these simulations was used to create a virtual experience of these spaces using Ambisonics.

1.3 Previous works on the theatre of Tindari

The work described in this thesis would not have been possible without the data and insights on the Theatre of Tindari gathered in more than six years of studies conducted by the Department of Energy of the Politecnico di Torino, directed by Arianna Astolfi and Louena Shtrepi and the thesis written on the subject by Eirini Kostara and Federica Lepore, 2015, Giovanni Augusto Bouvet, 2016, Elena Bo, 2017 and Giulia Benvenuto, 2020. Their contributions will be highlighted throughout the hole dissertation.

2. AMBISONICS

This Chapter introduces to the concepts and terminology that are necessary to understand the process simulation and auralization that will be the subjects of Chapter 6 and 7.

The first implementation was essentially based on similar considerations as Mid-Side recording (MS) a technique patented Alan Dower Blumlein in 1933 used on some of the earliest stereophonic recordings, with an added figure-of-eight microphone of up-down aiming (Zotter and Frank, 2019). This setup provided the what later would be called a First Order Ambisonics (FOA)

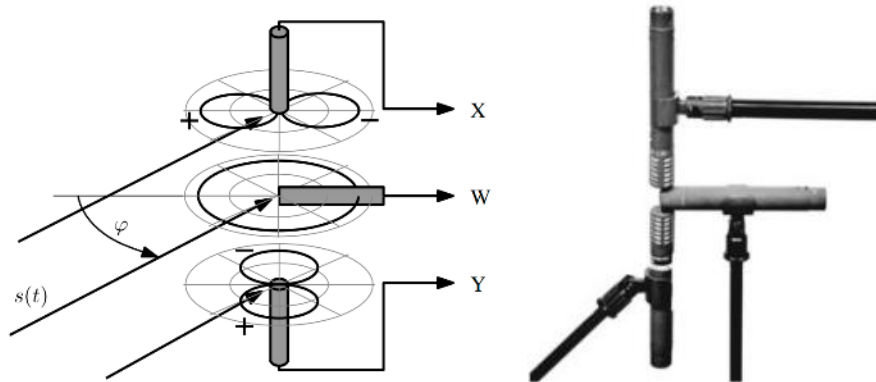


Figure 1: Native 2D first-order Ambisonic recording with an omnidirectional and a figure-of-eight (Zotter and Frank, 2019)

This is not however the typical configuration used today for FOA recording, e.g. one popular solution is the use of four cardioid microphones in a tetrahedral arrangement, known as a “sound field microphone”.

To understand how this method of recording can provide the directionality information of the whole sound field, although somehow blurred, we must introduce the concept of spherical harmonics.

2.1 Spherical harmonics

Spherical harmonics are three-dimensional orthogonal polar patterns that decompose the sound field into its directional components.

“Orthogonal” means that each spherical harmonic represents a unique directional characteristics of the sound field which is independent of the directional characteristic described by the other harmonics.

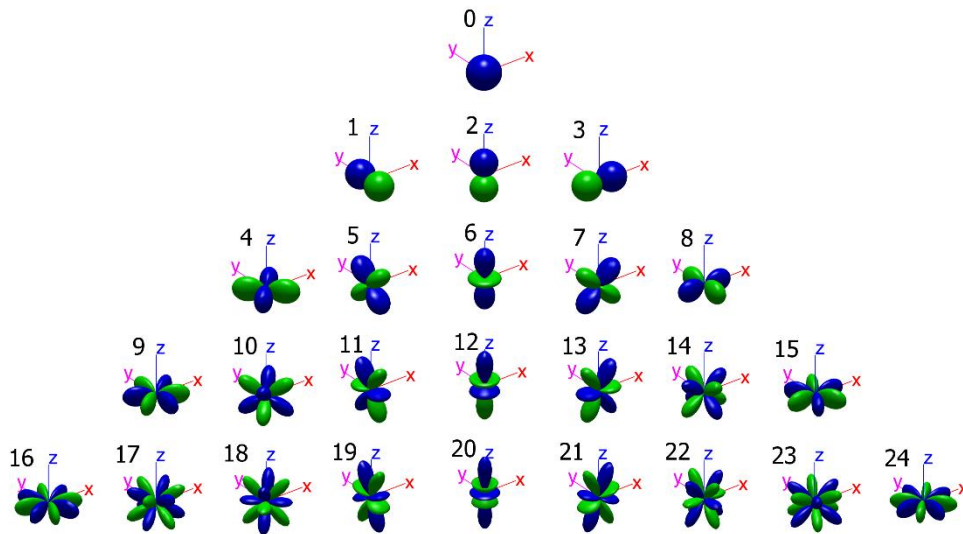


Figure 2: Spherical Harmonics in cartesian 3d space (Farina, 2017)

There are two common ways to represent real spherical harmonics in 3D. One is to use the basis function value as the radius in spherical coordinates (as in the picture above), the other one is using a heat map where the color represents the basis function value at a specific point on the sphere (as in the picture below).

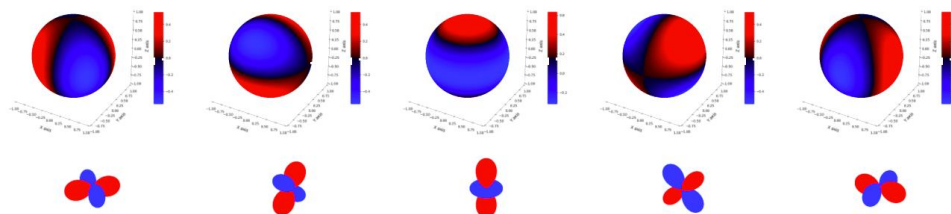


Figure 3: Comparison between spherical harmonics representations.
(Spherical Harmonic Basis Functions, 2021) Graphical elaboration by the author.

The decomposition of space into spherical harmonics can be described as a Fourier Transform on the surface of the sphere.

The Fourier Transform is a mathematical transform that decomposes functions depending on space or time into functions depending on spatial or temporal frequency ('Wikipedia', 2021). Its most common use is the decomposition of an audio signal into its individual spectral components.

Practically, in the case of spectral decomposition, it compares the signal's amplitude at time with a wave of a specific frequency, then if the correlation is high, that frequency band will get a proportionally high amplitude and if the correlation is low, it will get a low amplitude; then the process can be repeated with the next frequency and so on.

While in the typical use the considered domains are time and frequency, in the case of ambisonics the considered domains are space and spatial frequency (Noisternig, 2018).

Spherical harmonics are components of directionality as frequencies are components of a spectrum. In the same way, a higher degree of subdivision will provide higher resolution.

2.1.1 Ambisonic Orders

This means that increasing the number of spherical harmonics will increase the detail in the directionality of the sound field and allow for a better localization of the sound sources by the listener. In order to do that we must increase the Ambisonic Order (AO).

The AO and the quantity of spherical harmonics are related by a quadratic function:

$$n_h = (n_{AO} + 1)^2$$

n_h = number of spherical harmonics
 n_{AO} = number of ambisonic order

We could theoretically increase the order to infinity to get a closer and closer to the full description of the sound field, but many listening tests have proved that 4th order ambisonics can provide a good localization (Noisternig, 2018). The number of spherical harmonics also corresponds to the number of channels contained in the audio file, e.g. a 4th OA audio track will have 25 spherical harmonics and 25 audio channels.

2.1.2 Ambisonic ordering standards

The proper decoding an ambisonic file requires the knowledge of how the channels are ordered into the audio file.

Although it this approach was developed in the seventies and the techniques are well known, there are disagreements how to normalize, store and exchange Ambisonic data.

Two formats are in widespread use, the first is Furse-Malham (FuMa) higher-order format, although generally considered obsolete, and the more modern SN3D, in ACN channel order. ('Wikipedia', 2021)

			0			
		1	2	3		
	4	5	6	7	8	
9	10	11	12	13	14	15

			W_0			
		Y_2	Z_3	X_1		
	V_8	T_6	R_4	S_5	U_7	
Q_{15}	O_{13}	M_{11}	K_9	L_{10}	N_{12}	P_{14}

Figure 4: The ordering of ACN (to the left) and the ordering of FuMa (to the right)

2.1.3 Ambisonic Convolution

The uses of ambisonic are not limited to simple recording and playback, it can also be used obtain the spatial IR (Impulse Response) of a space by comparing a know anechoic input signal with the audio recorded by an omnidirectional receiver in the same space through a process called *convolution*.

Following the same principle we can use an ambisonic IR, in what's called *B-Format*, to convolve any anechoic sample and reproduce it as if it was played in room where the IR was registered. This technique will be later discussed in more detail later wile describing how it was applied in this study.

3. ARCHEOACOUSTICS: LITERARY REVIEW

3.1 Studies on the on ancient theatres

3.1.1 From Vitruvius to the Renaissance

Ancient open theaters always held a symbolic status in the architectural studies: in the first century BC, Vitruvius described them as “emendate”, “models without mistakes”, in the V book of *De Architectura*: in other words, perfect. (Bo, 2017)

Vitruvius recognized that what guided their designs were the rule of Nature, the harmonic relations that represented for him the foundations of architecture and the basic structure of the cosmos. He in fact dedicated an entire chapter to the concept of harmony, the *V Chapter: De Harmonia*.

Vitruvius describe for the definition of the theatrical plans, starts from the circle, called *perimetros imi*. Then, the dimension of the architectural elements derives from the modular division of its diameter, following these steps: a) definition of the *scaenae frons* limits, of the *proscenium* and *orchestra* width; b) of the stairs position, in-between *cunei* and the three scenic doors; c) in elevation, the *pulpitum*’s height. (Bo, 2017)

The treaties written by Vitruvius constituted a problem for architectural historians of all historical periods, because of their lack of any imagery¹.

The renaissance saw a great revival of interest his studies, with many architectural historian trying to delineate the canons that Vitruvius used to define the theatre’s geometries.

This was the beginning of centuries of studies that through the centuries got emancipated from the writing of Vitruvius to finally embrace a more scientific approach with Canac and later with the recent project ERATO.

Hereafter are mentioned some of most important of the renaissance period:

¹Some fonts report the existence of some illustration, but none has been found.

1. The *De Aedificatoria* of Leon Battista Alberti proposed alternative methods for assigning proportions than those presented by Vitruvius;
2. . The *Spectacula*, by Pellegrino Prisciani, represented the first treatise entirely dedicated to performance spaces;
3. The second book of *Tutte le opere di architettura et prospettiva*, written by Sebastiano Serlio, focused on the perspective and the visibility of the spectators; in the third book, on classical antiquities, he documented the ruins of the ancient theatres of Pola, Ferento, Roma, and othoers, with graphical reconstructions. (Bo, 2017)

3.1.2 The studies of Canac

In the 20th century, the advent of the Geometrical Acoustics (GA) was accompanied by a re-born interest for the ancient techniques of geometrical design of theatres. (Bo, 2017)

In 1967, after forty six years of studies on Greek and Roman thetres, Canac published *L'Acoustique des théâtres antiques: ses enseignements*, a book based on twenty years of archaeological and scientific research in France, Italy, Greece and Asia, titled (Canac, 1967).

François Canac combined historical and archeological research with acoustical analysis, he was pioneered the multidisciplinary approach that nowadays constitutes the basis of all studies in archeoacoustics.

The first of his contribution concerns the importance of the scene in ancient theatres. This study is important for two reasons: because, many of the Greek theater that presented a scene, including the Theatre of Tindari, don't have it anymore, therefore it's important to be conscious of the essential importance of this architectural element on sound characteristics of this spaces.

The other reason is that in this studies he contrived some very ingenious empirical solutions to be able to conduct advanced acoustic experiments with very limited instrumentation.

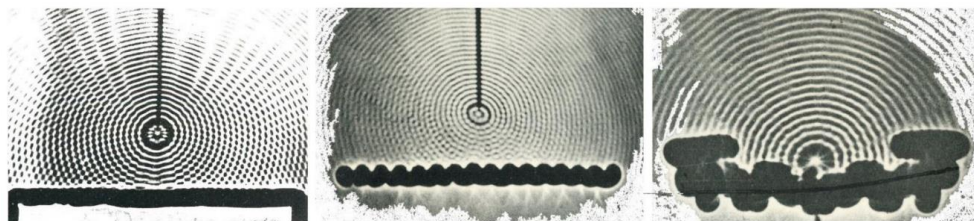


Figure 5: Study on sound propagation, reflections obtained with a plan wall (a), with an alveolar wall (b), and with the reproduction of the ancient theatre of Orange scaenae frons (c). Images from (Canac, 1967)

In the pictures above we can see some photos of his experiments with water: he immersed models of scenes, in scale 1:1000, with various surfaces in order to test their scattering power. Then he generated ripples on the surface of the water through the use of a small vertical rod linked to an electromagnet. The recordings of the reflections of the ripples on the models demonstrated that the complexity of the architectural elements of the façade have a strong impact on the diffusion of sound.

The other expedient that he pioneered is still used today: it consists in conducting acoustic tests on a small scale model with ultrasounds.

The general aim of his work was to assess how every element of the theatre contributed to the complex system of relations that bring the soundscape of open theatres to life.

With this purpose in mind he developed the seven “canonical equation” of ancient theatres. Describing the contributions of the main elements: the cavea, the scaenae frons, and orchestra, through the definition of geometrical rules. (Bo, 2017)

3.1.3 Project ERATO

ERATO is a project carried out by the European Commission from 2003 to 2006, it took its name from one of the nine Muses, the patron of lyric and erotic poetry.

The objectives of this project were the identification, Evaluation and Revival of the Acoustical heritage of ancient Theatres and Odeas. The project was developed in the framework of INCO-MED in 2003 – 2006 (Rindel, ERATO, Final report, 2006).

The project consisted in two main phases: in situ measurements, and reconstruction as virtual models of five ancient theatres: the theater of Aspendos (Turkey), of Jerash (Jordan), of Syracusae (Italy), and the ancient odeon of Aosta (Italy) and Aphrodisia (Turkey).

The study highlights how actual acoustical conditions of these architectures changed in time due to deterioration and the loss of architectural elements that were essential for their acoustic performance.

The revolutionary virtual approach allowed the comparison between the actual condition evaluated throughout measurements, and the hypothesized ancient conditions evaluated throughout simulations. This opened a debate on the correct use of simulation tools, which is still open today. (Bo, 2017)

It also stressed out the importance of the functionalization of this cultural heritage, in order to promote their conservation, and the important role that virtual reconstruction can play in that regard.

3.3 The ISO 3382-1:2009

The generally recognized reference to evaluate and compare ancient theaters is the same used for general performance spaces, that is the ISO 3382-1:2009 (this was not yet published during project ERATO, so the previous version, the ISO 3382:2000, was used in that case).

The lack of a distinction between open and closed performance spaces poses some problems, the use of T60, that is the time required for a signal emitted in a room (from an omnidirectional sound source) to decay over 60 dB, is not appropriate for spaces with such short IRs.

It is therefore necessary to use parameters indicated in the second note of the document, i.e. the T30, which considers the decay time for 30 dB, and more often the T20, which considers the decay time for 20 dB.

The decay curve can be obtained with the following equation:

$$E(t) = \int_t^{\infty} p^2(\tau) d\tau = \int_{\infty}^t p^2(\tau) d(-\tau)$$

p = pressure of the impulse response as a function of time

E = energy of the decay curve as a function of time

t = time

(ISO 3382-1:2009 'Measurement of room acoustic parameters - part 1: performance spaces.', 2009)

The document also defines other parameters that were taken into account during the analysis of ancient theatres, above all G, D50, C80, and STI.

G, the Robustness Index, represents the perceived level sound in a space compared to level perceived in an open field at a distance of 10m from the source. It is defined as the logarithmic ratio between the square root of the sound pressure of the impulse and the square root of the sound pressure measured at a distance of 10 m.

$$G = 10 \lg \frac{\int_0^{\infty} p^2(t) dt}{\int_0^{\infty} p_{10}^2(t) dt} = L_{pE} - L_{pE,10} [dB]$$

In which

$$L_{pE} = 10 \lg \left[\frac{1}{T_0} \int_0^{\infty} \frac{p^2(t) dt}{p_0^2} \right] dB$$

And

$$L_{pE,10} = 10 \lg \left[\frac{1}{T_0} \int_0^\infty \frac{p_{10}^2(t) dt}{p_0^2} \right] \text{dB}$$

$p(t)$ = is the instantaneous sound pressure of the impulse response measured at the measurement point.

$p_{10}(t)$ = is the instantaneous sound pressure of the impulse response measured at a distance of 10 m in a free field.

p_0 is 20 μPa

$T_0=1$ s

L_{pE} = s the sound pressure exposure level of $p(t)$

$L_{pE,10}$ = is the sound pressure exposure level of $p_{10}(t)$

(ISO 3382-1:2009 'Measurement of room acoustic parameters - part 1: performance spaces.', 2009)

D50 stands for “definition”, it describes the early-to-late arriving sound energy ratio. It is defined as the logarithmic ratio between the sound energy arriving to the receiver during the first 50 seconds after the initial transient and energy received after that threshold.

The early energy is considered “useful” because it is perceived as an increment of loudness, the late energy is considered disturbing.

This parameter usually relates to conditions for speech.

D50 is also referred to as C50, and so it will be called in this thesis in order to conform to the previous studies on the theatre of Tindari.

$$C50 = 10 \log \frac{\int_0^{50\text{ms}} p^2(t) dt}{\int_{50\text{ms}}^\infty p^2(t) dt} [dB]$$

C80, Clarity is similar to C50 with the only difference that the threshold between early and late energy is set at 80ms. This is useful in order to evaluate the conditions for musical performances.

$$C80 = 10 \log \frac{\int_0^{80\text{ms}} p^2(t) dt}{\int_{80\text{ms}}^\infty p^2(t) dt} [dB]$$

Another useful parameter is STI, Speech Transmission Index, an adimensional index of the intelligibility of speech, its value can go from 0 to 1. A STI of 0.5 or higher is generally consider sufficient for a good intelligibility.

Although the spoke word was primary destination of use of the open air theatre, this parameters was not considered useful for the process of calibration.

The ISO 3382-1:2009 also define the JND, Just noticeable difference for all the parameters above mentioned.

JND is a term derived from experimental psychology, it defines the amount how much a parameter has to change in order for a difference to be noticeable, detectable at least half the time. ('Wikipedia', 2021)

The table in the following page shows the JND for every parameter defined in the document, it also briefly define some of the parameters that were not taken into consideration in this dissertation.

	Acoustic quantity	Subjective listener aspect	JND	Typical range ^a
<i>Temporal</i>	Reverberation Time, RT, (s)	Reverberation	Rel. 5%	1.8 ÷ 2.2 s
	Early Decay Time, EDT, (s)	Perceived Reverberation	Rel. 5%	1.0 ÷ 3.0 s
<i>Energetic</i>	Definition, D ₅₀ , (dB)		0.05	0.3 ÷ 0.7
	Clarity, C ₅₀ (dB)	Perceived Clarity of sound	1.1 dB	≥ 0 dB
	Clarity, C ₈₀ , (-)		1 dB	-5 ÷ +5 dB
	Centre Time, T _s , (ms)		10 ms	60 ÷ 260 ms
	Sound Strength, G, (dB)	Subjective Level of sound	1 dB	-2 ÷ +10 dB
<i>Spatial</i>	Early Lateral Energy Fraction, LF ₈₀ , (-)	Apparent Source Width (ASW)	0.05	0.05 ÷ 0.35
	Inter-Aural Cross Correlation Coefficient, IACC, (-)	Spatial impression	0.075	0.2
	Speech Transmission Index, STI, (-)	Speech Intelligibility	0.05	0.60 ÷ 0.75
	^a Frequency-averaged values in single positions in non-occupied concert and multi-purpose halls up to 25.000 m ³			

Table 1: Acoustic qualities and corresponding subjective listeners aspects (Bo, 2017)

4. Framework of the case study

4.1 Territorial framework

The ancient city of Tyndaris is located on a spectacularly sited promontory, 180 meters above the bay of the Tyrrhenian Sea on the northern coast of Sicily. The city was founded in 396 BCE by the Greeks as a colony for exiles of Messenia (modern Messina), who had been forced out of the Peloponnesian Peninsula. The site is 59 km from Messina and is bounded by the Punta di Milazzo on the east, and the Capo Calavà on the west. (Hines, 2019).

The urban layout of the city probably remained the same from its foundation up to the imperial era, it had a regular fabric intelligently adapted to the geomorphology of the site, with blocks, or *insulae*, of 30x78 meters, defined by the orthogonal intersection of three main *decumani* that ran from south-east to north-west, each eight meters wide, with a series of smaller transverse roads, the *cardines*, each three meters wide. (Benvenuto, 2020)

Nowadays the theatre is surrounded by a rich archaeological park containing Roman habitations and baths, complete with wonderful floor mosaics and a small but well presented museum. Further on is the Basilica, a fine example of Graeco-Roman architecture (Hines, 2019). The theatre is still hosting theatrical plays and concerts, but their acoustic quality is threatened by increasing background noise level, due mainly to traffic.

Location:	Modern Tindari, Province of Messina, Sicily, Italy
Theatre Type:	Greek Theatre with Roman Additions
Date of Construction:	4th c. BCE
GPS Coordinates:	38.14377, 15.04234
Dimensions:	Cavea Width: 76 meters Orchestra Diameter: 23 meters
Seating Capacity:	3,000

Table 2: Basic information about the theatre of Tindari



Figure 6: General Plan in scale 1:5000, courtesy of Parco Archeologico di Tindari (2020). Graphical elaboration by the author

4.3 Historical framework

“The interest that the theatre of Tindari presents in the history of ancient architecture by far transcends the topographical sphere, due to the fact that its monumental “Scaenae frons”, of which conspicuous elements are preserved, constitutes, together with that of the theater of Segesta, the most significant precedent of the architecture of the scenic buildings of the Roman imperial age. Together with the theater of Segesta the theatre Tindari is the most evident document of an architectural tradition typical of Sicily and Magna Graecia in the Hellenistic period, of which much more vague and uncertain clues can be found in the theaters of Syracuse and Pompei” (Bernabò Brea, 1965) (translation by the author)

The theatre was built by the early Hellenistic founders of the city after 396 BC, and it was initially constituted only by the cavea, the skené was added later. Subsequently, in Roman times (around 22-21 BC) the theatre was transformed into an arena, so it had to be remodelled to make it more appropriate for blood sport entertainment. The level of the Greek orchestra was lowered of 0.90 m; the proscaenium and the four first rows of the theatre were destroyed and used to build a 2.50 m height podium. The Greek-Hellenistic scene remained untouched during the Roman period, but it collapsed in late-medieval age (Bo, 2017). The city was then destroyed during the Arab conquest in 9th century, and so theatre were abandoned.

The scenic building in its was brought to light shortly after the execution of the survey conducted by Domenico Lo Faso, Duke of Serradifalco in 1842, by the excavation executed by the Commission of Antiquities of Sicily in the years 1842 and 1845.

Two excavation and restoration campaigns, (G. Cultrera in 1938 and L. Bernabò Brea between 1960 and 1966), revealed the theatre ruins we see today. (Hines, 2019). Bernabò Brea also curated the graphical reconstruction of the previous configuration of the theaters that constituted the main reference for the creation of the acoustic model of the historical phases of the theatre discussed in Chapter 6. Some of his drawings are shown at the end of the current Chapter.

4.4 Current conditions of the theatre

The current acoustical performances of the theatre are compromised by many factors: the lack of the original scenic building, responsible of useful

reflections supporting the actor voice, the absence of a large part of the steps of the cavea and the general deterioration of the materials, impacting their reflectivity, and finally the increasing noise levels of the surroundings due to traffic.

New temporary seats have been added to welcome the public to experience this invaluable space, but an intervention on the acoustic behavior of the building is yet to be seen.

The usual approach chosen to solve the acoustic problems of open space theatres is compensate with electroacoustic systems. Although this choice is certainly an effective in tackling the low Robustness of these spaces, it also covers up the acoustic qualities.

Different solutions are possible, for example the construction of a temporary reflective scene, can provide an unintrusive and sustainable optimization of the acoustic performance. (Bouvet *et al.*, 2020)



Figure 7: Photo of the current state of the theatre of Tindari, taken during the measurement campaign of 2015 (curtesy of DENERG)

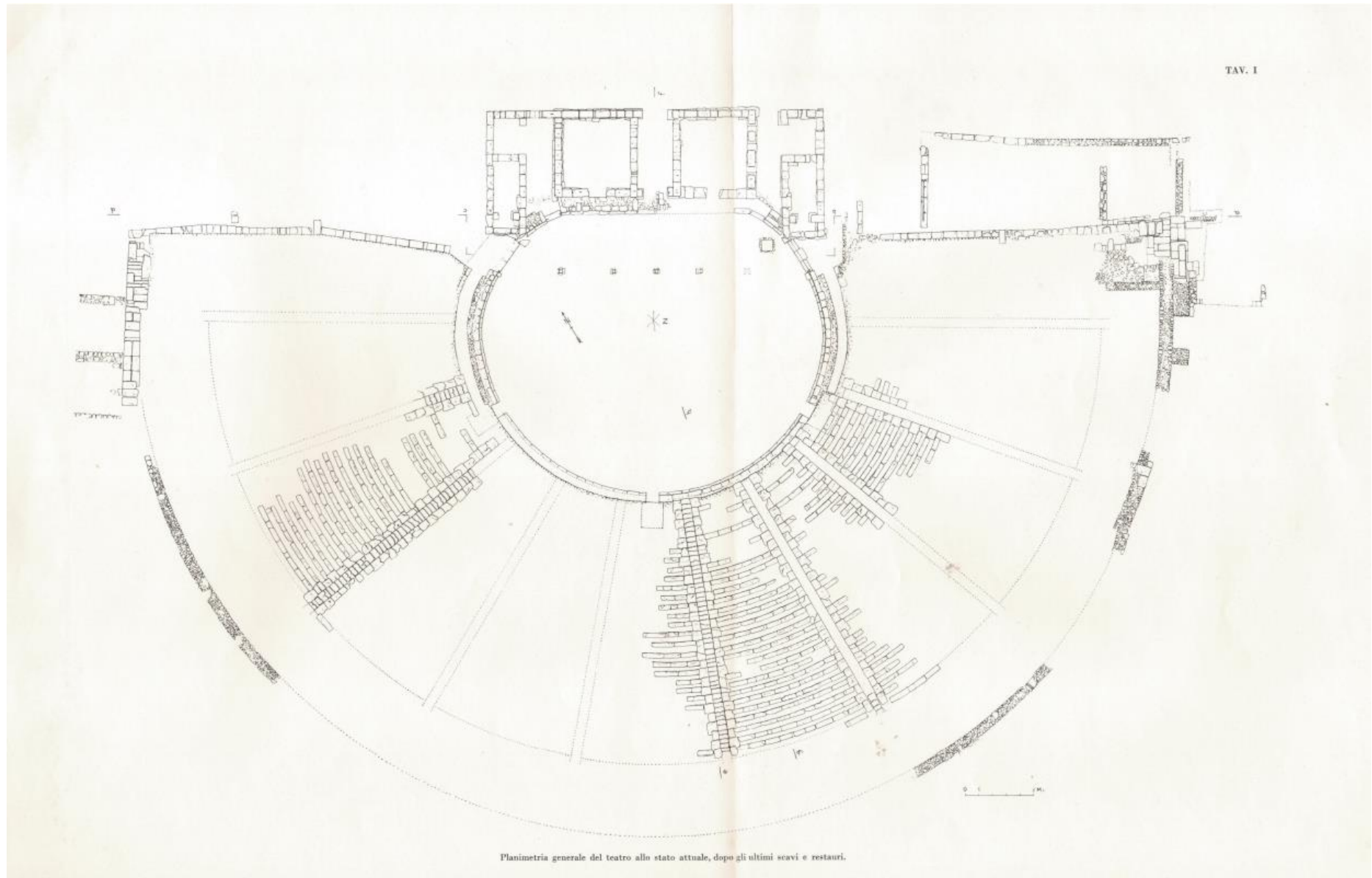


Figure 8: General Plan of the theatre after the restauration works of 1965 (Bernabò Brea, 1965).

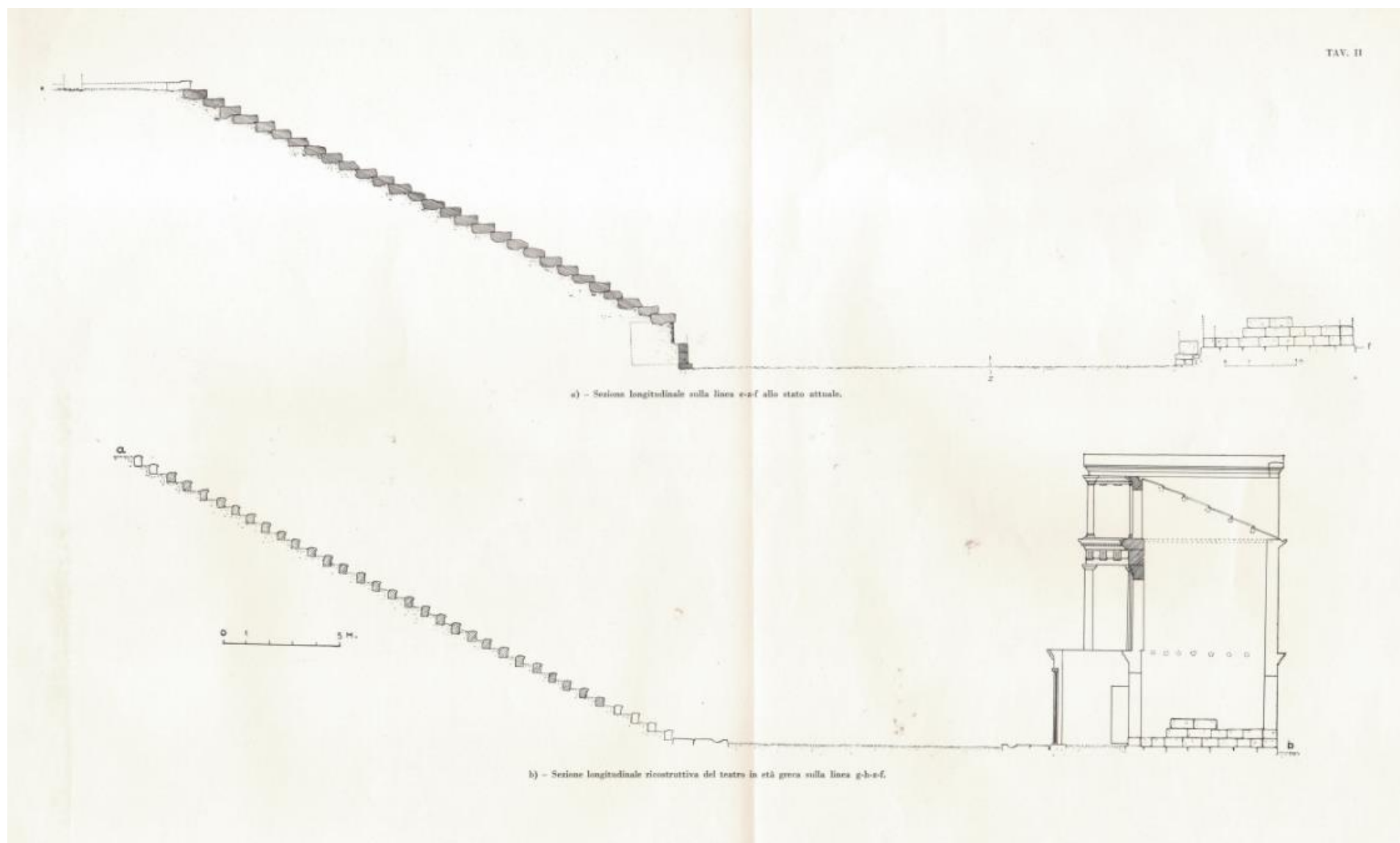


Figure 9: Longitudinal section of the theatre after the restauration of 1965 (above) and reconstructive section of the Hellenistic configuration (Bernabò Brea, 1965).

5. PREVIOUS WORKS ON THE THEATRE OF TINDARI

This chapter illustrates the evolutions of the analysis of the theatre of Tindari and proposes a critical analysis of their methodology, it also highlights the reasons that led to the choice of repeating the process of calibration creating a new model of the current deterioration state and then create new reconstructions of the historical configurations of the theatre.

5.1 The measurement campaign of 2015

In September 2015 the Energy Department of the Politecnico di Torino (DENERG) conducted a survey which became the basis of the following six years of studies on acoustics of the theatre of Tindari. The measurements were taken with three different omnidirectional sources in the orchestra.

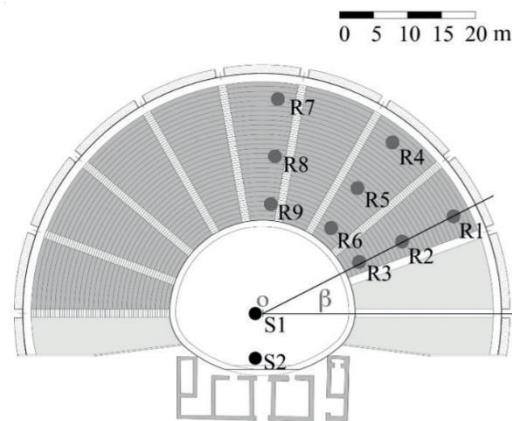


Figure 10: Measurement set-up: S1 and S2 indicate the source positions. R1–R9 indicate the receiver positions. O is the centre of the orchestra (at a distance of 1 m from S1, to the left, on the same horizontal axis) and β is the angle from the scenery line and the direction that joins the source and the receiver (Astolfi et al., 2020).

Two types of firecrackers were used to generate the sound impulse, specifically the "Raudo Manna New Ma1b " and the " Perfetto C00015 Raudo New "; the third source was and the dodecahedron "Briel & Kjaer Omnipower Sound Source 4296 " powered by a "Lab. Gruppen LAB 300" connected to a the laptop. The microphone used was a "Shoeps CMC 5-U". The data obtained with the two recordings were then analyzed with two different software: DIRAC and Adobe Audition (Astolfi *et al.*, 2020).

5.3 The simulation of the current state

The elaboration of an reliable model of the current state of the theatre can be chronologically divided by three milestones:

1. The Master thesis by Eirini Kostara and Federica Lepore, 2015, that presented the first calibration of a simple model of the current state of the theatre, obtained by comparing its EDT, T20, T30, G, C50 and C80 with the results corresponding values extracted by the analysis of the IRs obtained with the survey.
2. The Phd thesis by Elena Bo, 2017, that assessed the reliability of the model and tested it in a round-robin between two different raytracing software Odeon and Catt.
3. The Master thesis by Giulia Benvenuto, 2020, increasing the detail of the model both in its form and in the distribution and physical qualities of the materials.

The contribution of this works is not limited to the advancement of the model listed above, e.g. the thesis of Elena Bo presents an in depth analysis of the systematic and randomic errors of the GA simulations and compared the simulation of the theater of Tindari with her own simulation of the ancient theatre of Syracuse; the thesis of Giulia Benvenuto compared the acoustical parameters of Tindari with those of many other ancient theaters and proposed a reconstructive acoustical model of the previous configurations of the theatre (as will be seen in next Section).

Another work that should be mentioned is the master thesis written Giovanni Augusto Bouvet in 2016, that didn't contribute to the specific topic that we are discussing in this chapter, and will be covered in Chapter 6.

In this section we will summarize ho Giulia Benvenuto, building on the work of Elena Bo, realized the model that constitutes the main reference of this thesis. At the end of the chapter we will see why her reconstruction, although very valuable, was not considered suitable for the prosecution of the studies.

G.Benvenuto noticed that the first model of Lepore and Kostara Konstantinou of the theater was very simplistic in its geometry and materials, so exported the original Autocad model, whose main shape was generated parametrically in MATLAB, to SketchUp v2018 where she added more detail to the geometry and proceeded to a more differentiated and detailed mapping of the materials, based on the photos of the survey. (Benvenuto, 2020)

SketchUp is very well integrated with Odeon, the plugin SU2Odeon, makes the interoperability of these two software very agile, but still it doesn't compensate for the lack of control on the geometry characteristic of SketchUp, which can constitute a big problem in Geometrical Acoustics simulations (we will later see how made this model unusable for the prosecution of the studies).

Then she positioned a sound source to this coordinates: X=-1.00; Y=0.00; Z=1.70, and added a gain of 31 dB to the strength of its signal.

The coordinates of the receivers is shown in the next page.

No	x	y	z
1	28.34	13.75	11.9
2	20.79	10.08	7.7
3	14.39	7.19	4.2
4	18.97	25.15	11.9
5	13.91	18.44	7.7
6	9.69	12.86	4.2
7	2.65	31.39	11.9
8	1.95	23.02	7.7
9	1.35	16.04	4.2

Table 3: Coordinates of the Receiver in the calibration model of Giulia Benvenuto. Graphical elaboration by the author

The following parameters where taken into consideration: EDT, T30, T20, G, D50 e C80, but the only two parameters that proved useful for the calibration process where T20 and G.

Thes two parameters became the ground for comparison of the IRs obtained with the survey and the IRs generated by the simulation, using the method of the Mean Absolute Difference (MAD), i.e. by comparing the average in absolute value of the parameters obtained between 500 and 1000 Hz for all receivers with the JND values according to ISO 3382-1: 2009. (Benvenuto, 2020).

The MAD method is very convenient to check the validity of a model, but it only takes into account the mid-range of the spectrum, ignoring the lows, the mid-lows, the mid-high, and the high; it is then unable to describe the correspondence of the tonal characteristics, in the opinion of the author.

The choice of the materials took into account the coefficients used for the previous simulations and compared them with those used for simulations of theaters, for example those presented at the 2011 conference in Patras for the ERATO project. It also took into account scientific articles by Yang, H.S., Kang, J., Cheal, C., concerning the absorption and scattering coefficient of vegetation, since part of the cavea is covered by grass. (Benvenuto, 2020)

The resulting map (shown in the next page) is certainly a step forward from the basic distribution of the previous works, but a more in-depth analysis reveals some major inaccuracies that constitute a valid reason to repeat the process of mapping from scratch for the new analysis they are object of this thesis.

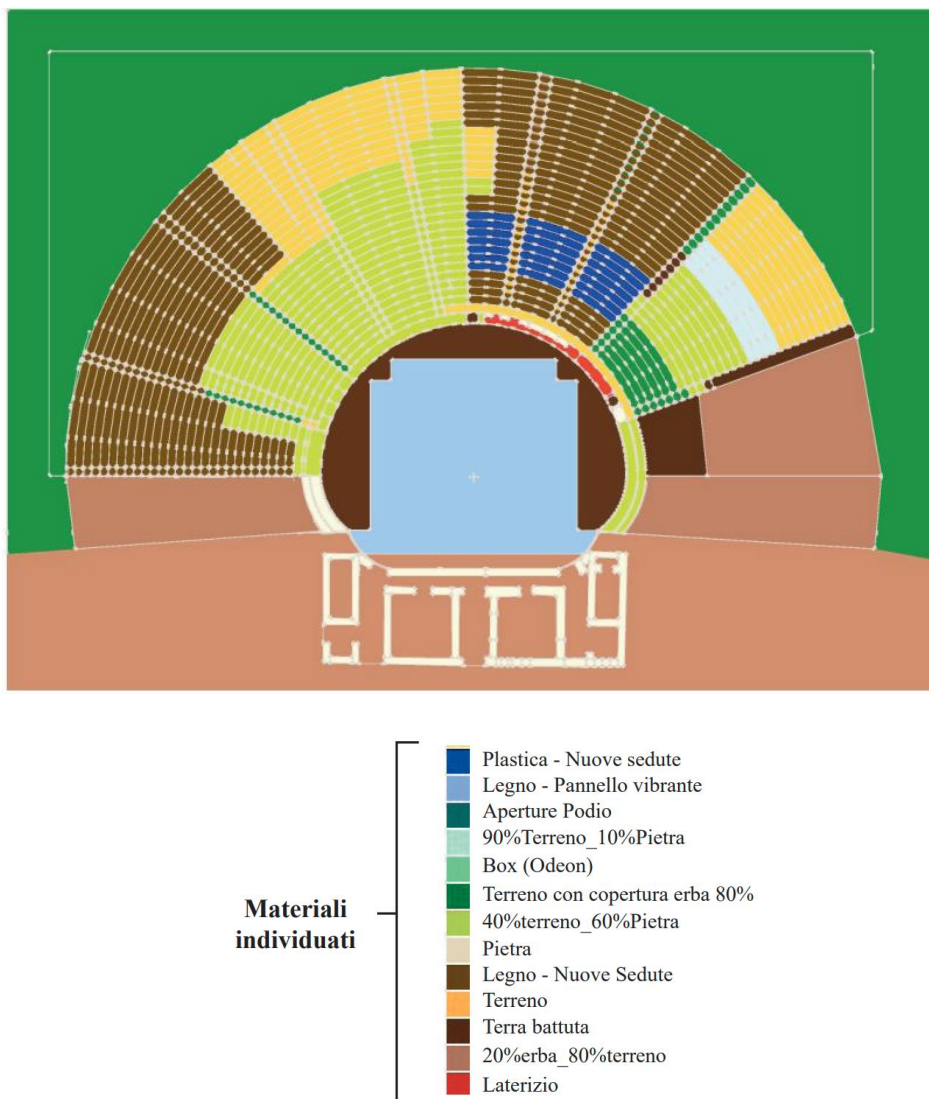


Figure 11: Sketchup view with the materials assigned by G. Benvenuto for her calibration model (Benvenuto, 2020)

MATERIALI	Frequenze (Hz)								Scattering
	63	125	250	500	1000	2000	4000	8000	707 Hz
ELEMENTI TERRA	0,25	0,35	0,42	0,43	0,44	0,3	0,21	0,19	0,8
PANNELLO VIBRANTE_LEGNO	0,4	0,4	0,3	0,19	0,03	0,03	0,03	0,03	0,3
PLASTICA	0,15	0,15	0,15	0,15	0,05	0,05	0,05	0,05	0,9
90%TERRENO_10%ERBA	0,24	0,33	0,39	0,41	0,36	0,25	0,12	0,08	0,52
20%ERBA_80%TERRENO	0,39	0,35	0,38	0,39	0,3	0,2	0,13	0,08	0,63
60%TERRENO_40%PIETRA	0,31	0,25	0,28	0,29	0,2	0,15	0,1	0,1	0,66
ERBA	0,2	0,25	0,36	0,37	0,38	0,28	0,19	0,18	0,1
PIETRA	0,1	0,1	0,1	0,1	0,1	0,1	0,1	0,1	0,55
TERRA BATTUTA	0,25	0,22	0,35	0,35	0,22	0,18	0,1	0,05	0,8
LEGNO	0,4	0,4	0,3	0,2	0,04	0,02	0,02	0,02	0,2
LATERIZIO	0,2	0,2	0,2	0,1	0,05	0,05	0,05	0,05	0,7
APERTURE PODIO	1	1	1	1	1	1	1	1	0,05

Table 4: absorption and scattering coefficient of materials assigned by G. Benvenuto for her calibration model (Benvenuto, 2020)

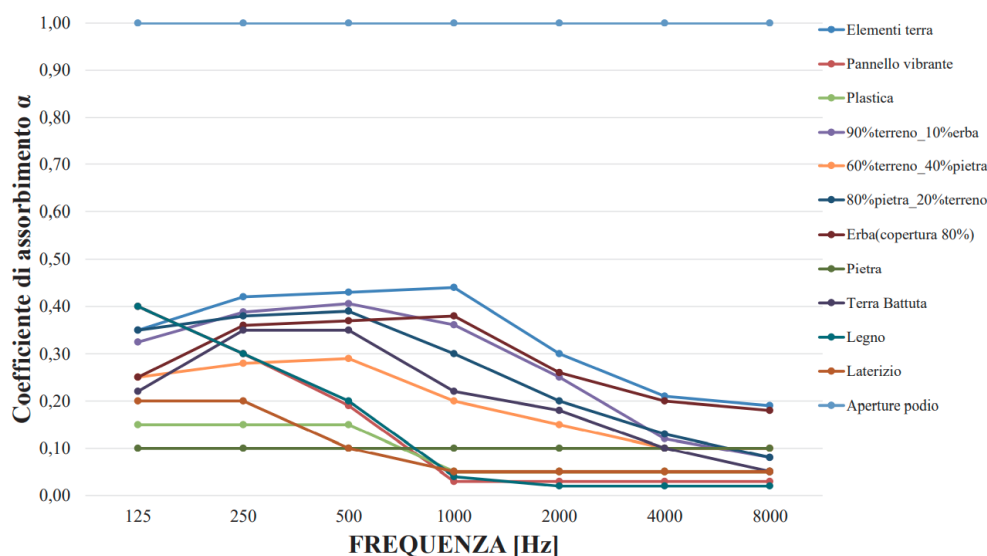


Table 5: diagram of the absorption coefficient of materials assigned by G. Benvenuto for her calibration model (Benvenuto, 2020)

The diagram above shows how the process of calibration brought to higher absorption levels for the lower frequencies and relatively low absorption for the high part of the spectrum: however this was not enough to validate the T20 for the frequency band of 125 Hz, as can be seen in a comparison with the T20 obtained from the measurement with one of the sources used for the survey, the dodecaedron, in Table 9. Both G. Benvenuto and E. Bo explain that this is probably due to the low reliability of the measurement for that frequency band, due to a INR (impulse to noise ratio), illustrated in table 6.

INR > 35 dB								
Theatre and Source	Frequency (Hz)							Average 500- 1000
	125	250	500	1000	2000	4000	8000	
TYN – S1 _D	69%	100%	96%	100%	100%	100%	100%	98%
TYN – S2 _D	64%	100%	100%	100%	100%	100%	100%	100%
TYN – S1 _F	65%	100%	100%	100%	100%	100%	100%	100%
SYR – S1 _F	64%	96%	100%	100%	100%	100%	100%	100%
SYR – S2 _F	100%	100%	100%	100%	100%	100%	100%	100%

INR > 45 dB								
Theatre and Source	Frequency (Hz)							Average 500- 1000
	125	250	500	1000	2000	4000	8000	
TYN – S1 _D	0%	62%	73%	65%	81%	62%	89%	69%
TYN – S2 _D	0%	64%	91%	91%	91%	73%	100%	91%
TYN – S1 _F	20%	100%	100%	100%	100%	100%	100%	100%
SYR – S1 _F	82%	46%	96%	96%	96%	96%	100%	96%
SYR – S2 _F	45%	100%	100%	100%	100%	100%	100%	100%

Table 6: Percentage of the measured IRs exceeding a certain decay range of INR (E.Bo, 2017)

After a trial and error of many material configurations and absorption coefficients, G.Benvenuto managed to verify the MAD for T20 and G, obtaining a deviance of 0,018 for T20, lower than the JND of 5% required in ISO 3382-1: 2009, and a deviance of 0,624 for G, lower than JND of 1 dB imposed by the standard.

The results of the MAD and T20 are shown in the next page. More results, i.e the values of C50 and C80 will be shown in Chapter 6 in comparison to the values obtained in the new simulations conducted by the author.

SIMULATO-MUSURATO_MAD T20 in frequenza								
	63	125	250	500	1000	2000	4000	8000
R1	0,29	0,14	0,03	0,03	0,00	0,01	0,02	0,04
R2	0,17	0,09	0,07	0,02	0,03	0,02	0,01	0,00
R3	0,07	0,01	0,02	0,01	0,03	0,07	0,08	0,07
R4	0,21	0,15	0,01	0,01	0,00	0,02	0,02	0,00
R5	0,22	0,03	0,03	0,01	0,00	0,01	0,04	0,04
R6	0,07	0,06	0,06	0,01	0,03	0,03	0,03	0,02
R7	0,24	0,00	0,02	0,00	0,02	0,02	0,03	0,03
R8	0,29	0,04	0,03	0,02	0,06	0,05	0,05	0,02
R9	0,09	0,13	0,03	0,04	0,00	0,06	0,05	0,02
media in frequenza	0,18	0,07	0,03	0,02	0,02	0,03	0,03	0,03
				Media 500-1000Hz		0,018		

Table 7: : Validation of the T20 of the calibration model of 2020 with the MAD method (Benvenuto, 2020)

SIMULATO-MISURATO_MAD G in frequenza								
	63	125	250	500	1000	2000	4000	8000
R1	3,02	2,14	0,90	0,51	0,24	1,52	2,26	5,15
R2	4,47	4,32	0,65	0,59	1,24	0,53	0,93	1,95
R3	3,87	2,75	0,06	1,28	0,56	1,38	1,63	1,35
R4	4,10	3,94	1,01	0,92	0,16	1,07	1,18	5,05
R5	4,00	3,97	0,95	1,00	0,05	0,94	1,36	3,25
R6	4,42	3,37	0,10	0,50	0,21	1,26	0,56	1,35
R7	5,35	4,41	0,61	0,79	0,27	2,69	1,75	5,00
R8	4,74	4,18	0,74	0,85	0,22	1,59	1,26	3,15
R9	5,60	4,43	0,80	0,48	1,40	0,71	0,24	0,15
media in frequenza	4,40	3,72	0,65	0,77	0,48	1,30	1,24	2,93
				Media 500-1000Hz		0,624		

Table 8: : Validation of the G of the calibration model of 2020 with the MAD method (Benvenuto, 2020)

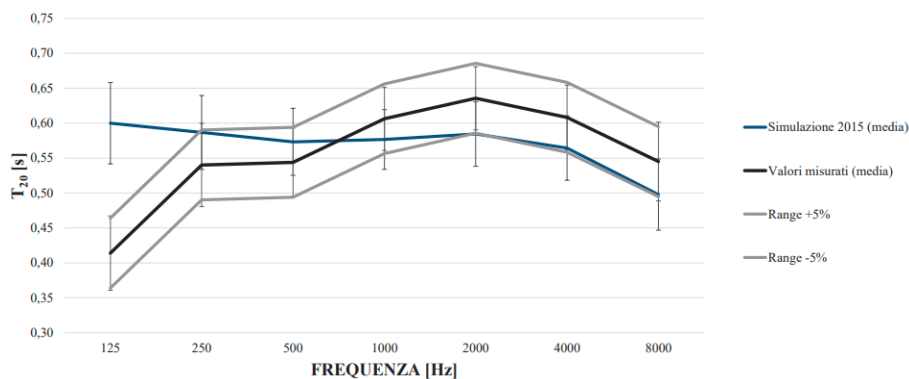


Table 9: Results of T20 for the calibration model of Giulia Benvenuto compared to the T20 obtained from the measurement with the dodecaedron.

5.4 Reconstruction of the historical phases

The other main contribution of the thesis of G. Benvenuto was to create the acoustical models of all the historical configurations of the theatre, based on the book "*Due secoli di studi, scavi e restauri del teatro greco di Tindari*" written by Bernabò Brea, L. in 1965 to sum up all the documentation and graphical reconstructions of the theatre of Tindari.

As stated by G. Benvenuto "To be able to compare the results with measurements of the current condition requires that the geometry, the points chosen for the positioning of the sources and receivers, and the environmental settings coincide in all models used for simulations".

This constitutes the first of many problems of these simulations, although the coordinate of Source and Receiver are the same, the point of origin of the geometry is different. In fact origin point of the reconstructive models was positioned in the geometrical center of the cavea, while in model she used for the calibration, originally modelled by Elena Bo, the geometrical center of the cavea is 1.52 meters away from the origin.

The second problem is that the dimensions of the orchestra (18,86 m) don't seem to match the reconstruction made by Bernabò Brea. Following his essay (as will be seen in next Chapter) leads to a diameter of 23.5 meters.

The shape of the cavea is also not correct, in fact "The fronts of the koilon's wings were not straight, but broken off at an obtuse angle having the vertex almost exactly half of their length"(Bernabò Brea, 1965).

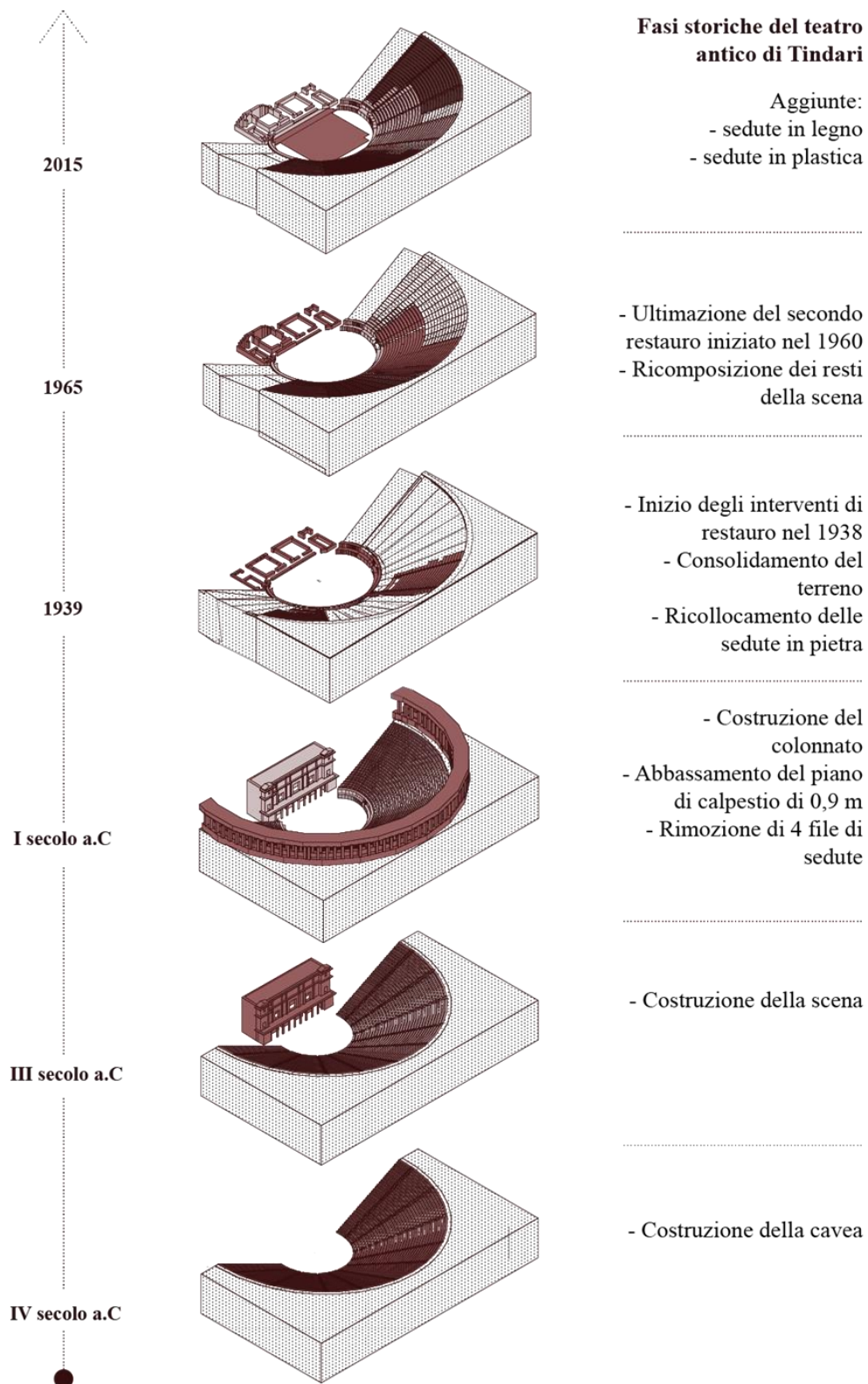
The original parodoi were very tight, they were even considered inexistent by the reconstruction of Von Gerkan in 1921; Bernabò Brea states that they were 1.1 meters wide, just enough to allow for the access of the public to the orchestra. In the reconstruction of G. Benvenuto they are 5.24 meters wide, far off from any previous assumption.

This results in a much smaller cavea, whose shape is comparable to the one proposed in the pictorial representations by Houel (1782), later contradicted by the excavations of the 20th century.

The dimensions of frons scaenae the frons scaenae are also not verified by the comparison with the documentation.

The results of these simulations will be compared to the new ones made by the author in the next Chapter.

Figure 12: (next page) Reconstruction of the historical phases of the theatre (Benvenuto, 2020)



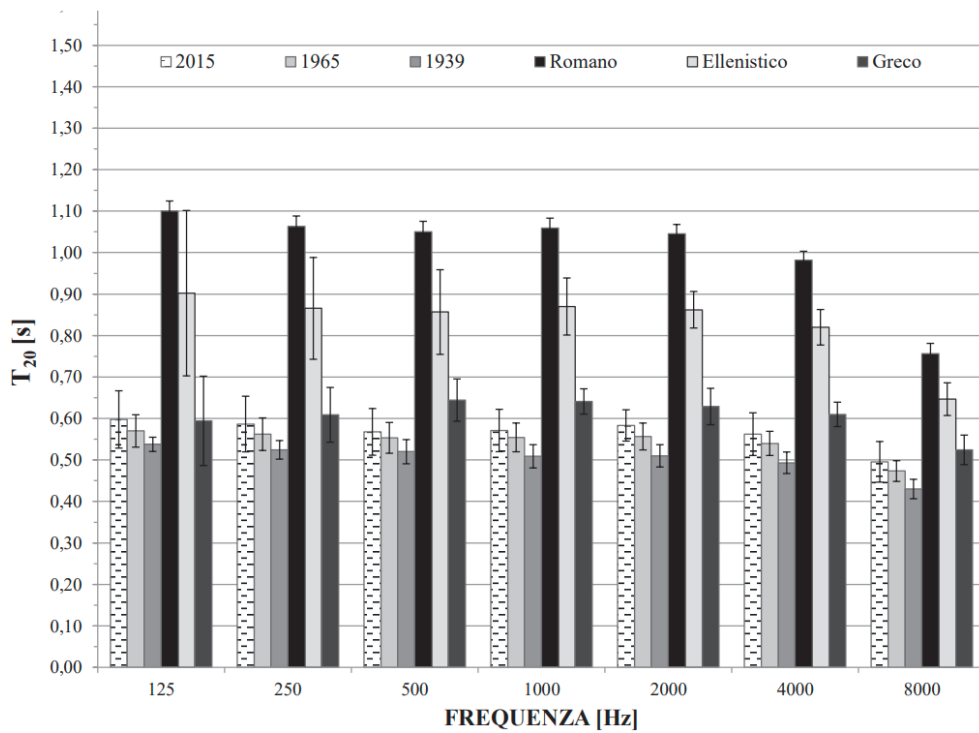


Table 10: Comparison between the T₂₀ of the different historical configurations per octave band (Benvenuto, 2020)

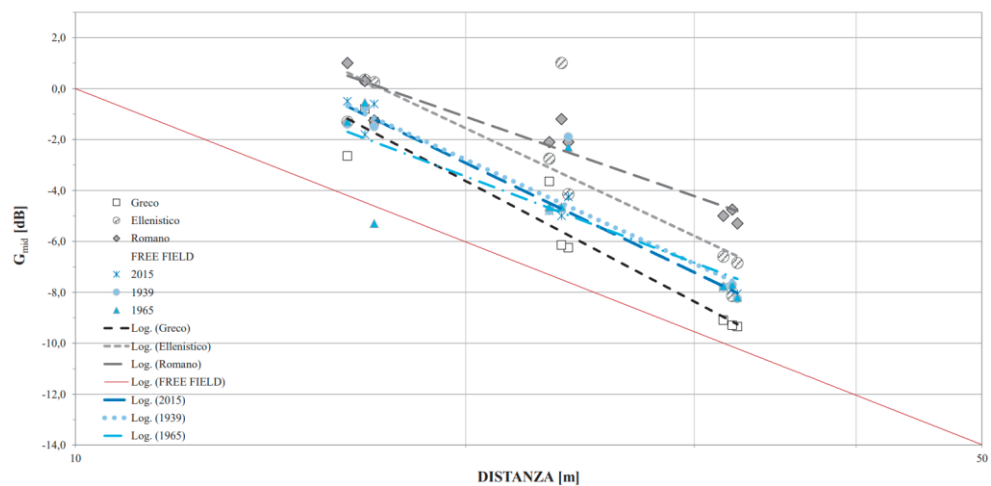


Table 11: Comparison of G_{mid} between 500 e 1000 Hz for every receiver for the different historical configurations (Benvenuto, 2020)

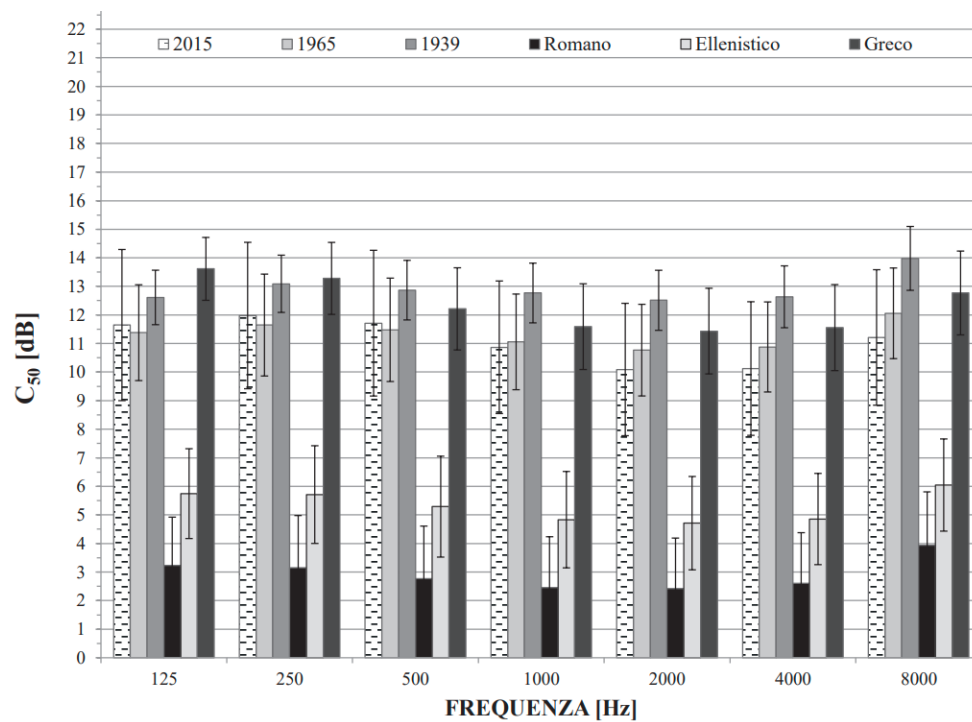


Table 12: Comparison between the C₅₀ of the different historical configuration per octave band (Benvenuto, 2020)

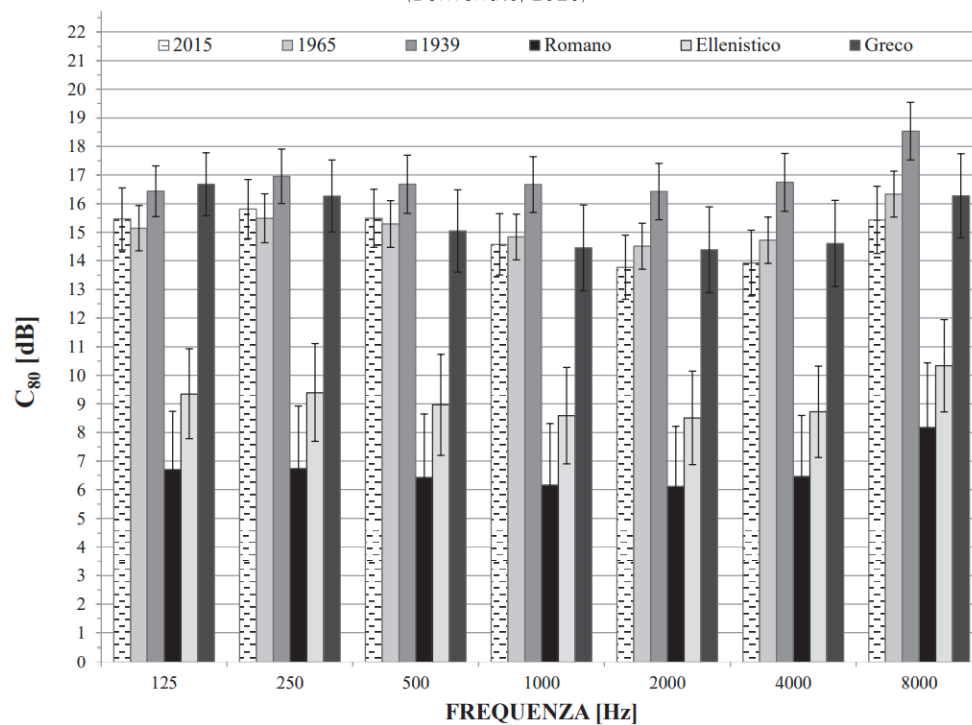


Table 13: Comparison between the C₈₀ of the different historical configurations (Benvenuto, 2020)

6. METHODOLOGY AND RESULTS

This chapter describes how, building on these bases of the previous studies, new work has been conducted in order to further improve the accuracy of the calibration model, and to test its reliability in a round-robin between two software based on a different GA method, Odeon and Ramsete.

All the results will be compared to the values obtained from the measurement campaign of 2015 and from the simulations conducted by G.Benvenuto in 2020.

6.1 Comparing Odeon and Ramsete

Both of these software are based on Geometrical Acoustics, but they use different tracing methods: while Odeon uses an hybrid-raytracing algorithm, Ramsete uses Pyramid Tracing. In the followings sections we explain the principles of these two methods, their similarities, and their differences.

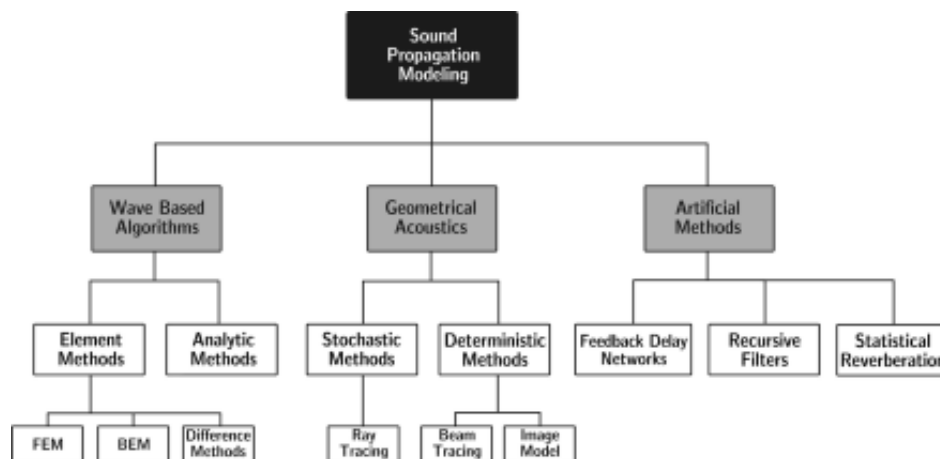


Figure 13: Categorization of the acoustic modelling methods by M.Vorländer.
The more recent Finite-difference time-domain method (FDTD) is missing from the list.
(Vorländer, 2020)

6.1.1 Odeon's Hybrid-Raytracing

The hybrid method of odeon consists in differentiating the early rays, calculated with the deterministic Image Source Method (ISM), and the late rays, calculated with ray radiosity (RRM), which is a statistical method since the rays will propagate for the source with random directional, making every simulation slightly different.

To account for early scattered rays, odeon uses the Early Scattering Method (ESM): for each image source that is generated with ISM, and that is visible to the receiver, a range of early secondary sources is generated on the surface the image source corresponds to. These early secondary sources, whose quantity is defined in the setting of the room, will emit early scatter rays. (Christensen, Koutsouris and Gil, 2020).

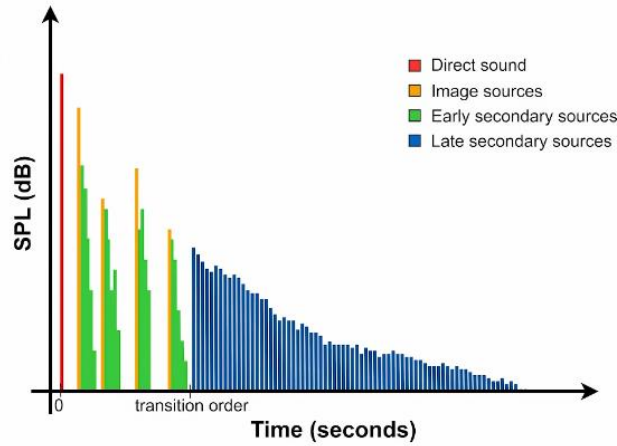


Figure 15: Representation of the contributions of ISM, ESM and RRM to the generation of the IR. Relation between Sound Pressure Level and Time. (Christensen, Koutsouris and Gil, 2020)

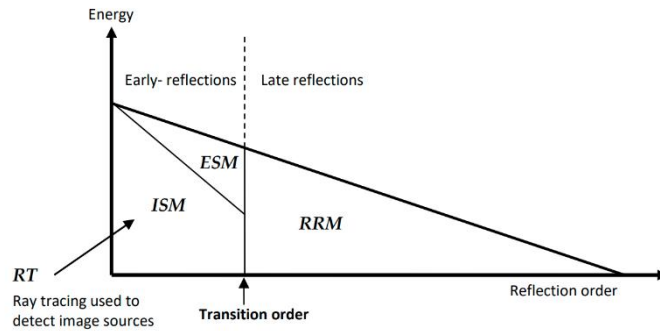


Figure 14: Representation of the contributions of ISM, ESM and RRM to the generation of the IR. Relation between Energy and Transition Order. (Christensen, Koutsouris and Gil, 2020)

The ISM and ESM are only used up to a certain limit called Transition Order, defined by the user, this is needed in to avoid the exponential growth calculation time, since the location of Image Sources is very demanding on the cpu, and it is an acceptable sacrifice on accuracy since specular energy becomes less important at higher reflection orders.

The proper value for the TO varies based on the dimensions and the geometrical complexity of the model. Here are some guidelines for a correct evaluation of the TO needed:

TO = 0 for volumes characterized by large curved (cathedrals, mosques) or for 3d models with an high number of surfaces.

TO = 1 for environments characterized by complex volumes, such as opera theatres, in this case the number of surfaces that define the mode should not be over 1000-2000.

TO = 2 for relatively simple rooms that can be modelled with a limited number of surface (50-100).

TO = 4 for basic geometries modelled with 20 to 50 surfaces.

6.1.2 Ramsete's Pyramid Tracing

Pyramid tracing in a GA method based on beam tracing, designed evolution of the of conical beam tracing. The main difference is that instead of propagating conical beams from the source, it radiates pyramids with three sided faces.

If we imagine an ideal sphere surrounding the source, its volume is completely covered by the pyramids without any overlapping, this is not possible with conical beams and leads to problems of multiple detection.

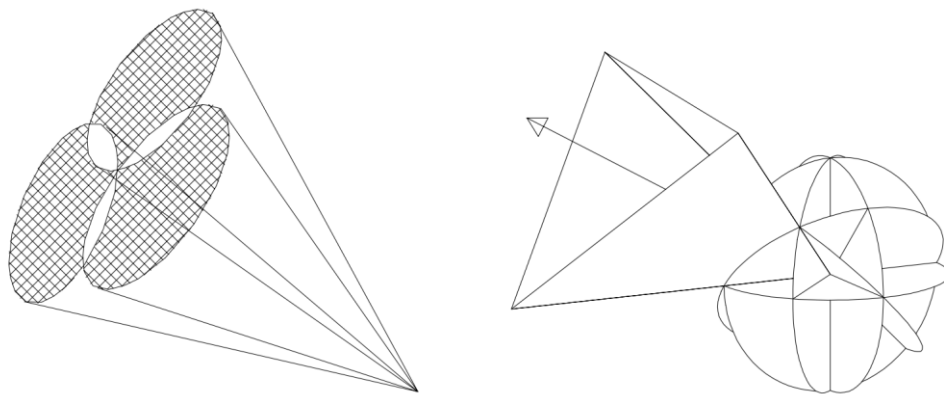


Figure 16: Comparison between beam tracing methods:
Cone Tracing (left) and Pyramid Tracing (right)

Unlike Odeon, Ramsete cannot be considered an hybrid room acoustical model because no distinction is made between *early* deterministic part of the Impulse Response and *late* statistical part, although for times larger than the critical one, the behavior of the acoustic field is estimated only from just a fraction of the “true” total number of arrivals (Farina, 1995).

Increasing the subdivision level makes the critical time larger; if it becomes larger than the length of the impulse response, then the tracing process can be considered purely deterministic.

Another difference is that the problem of the arbitrary dimension of the receiver is not present in Ramsete, since beam tracing makes it possible to use an adimensional point instead of a volume.

Beam tracing also provides much faster calculation time compared to raytracing.

Concerning the auralization potential of the two software, Ramsete offers much higher directional definition: while Odeon allows the creation of impulse responses in B-format up to the third ambisonic order, Ramsete allows can reach up to the fifth ambisonic order.

Practically the auralizations made with Odeon will consist of 16 channels, while those of Ramsete will reach up to 36, offering a significant increase in the detail of the sound field. Furthermore, the Odeon manual advises against the use of this software for auralizations beyond the first ambisonic order, having ascertained that, if in principle the 2nd and 3rd order should guarantee greater detail, the current development of the algorithm used returns a "fuzzy" sound field.

6.2 The creation of the new model

The first simulation in Ramsete was conducted on the model developed by G.Benvenuto in 2020. The result was a T30 that almost reached 1 second, and the IR showed numerous high energy echoes even two seconds after the initial transient. It was then clear the creation of a new model was needed as the topology of the mesh was incompatible with Ramsete's pyramid tracking method.

The high number of polygons, in addition to making the model less controllable, causes the program to generate an excess of bounces on of the individual rays, which affects the generation of the impulse response by extending it considerably.

Some three-dimensional modeling programs, such as Blender and 3ds Max, offer an automatic retopologization that reduces the polygon count, however this practice is not recommended for acoustic simulations and does not reach the level of geometric synthesis recommended.

A new cavea was then modeled in Ramsete CAD and exported in .dxf format to be further processed in Autocad, where the model was finalized. Then the same model was imported to both Odeon and Ramsete.

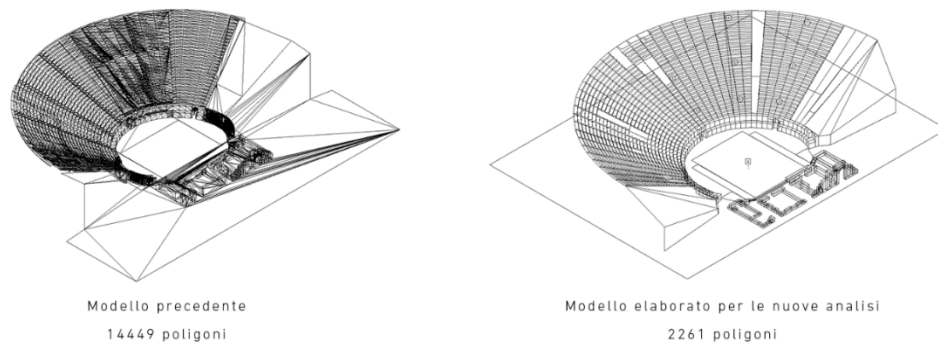


Figura 1 Axonometric visualization of the Sketchup model used in 2020 (right) and of the Autocad model used for the new simulations (left)
(Elaboration by the author on the model granted da G.Benvenuto)

The modeling was performed seeking a correct balance between accuracy and synthesis, without therefore going to an excessive level of detail, which would render the results unreliable simulation, but compensating for the simplification of the shapes with an increase in the scattering coefficient of the surfaces.

This significantly shortened the calculation times of the two programs and allowed greater control during the calibration phase.

Some big differences are noticeable between the two models, the most relevant is that the wings of the old cavea are perfectly aligned with the façade of the scaenae frons and are more then five meters afar from il, truncating a large portion of the theatre. The dimensions of the ruins of the scene had a surprising impact on the acoustical parameters because they generated late reflections with high energy, due to their low absorbance ($a=0.1$ for the hole spectrum).

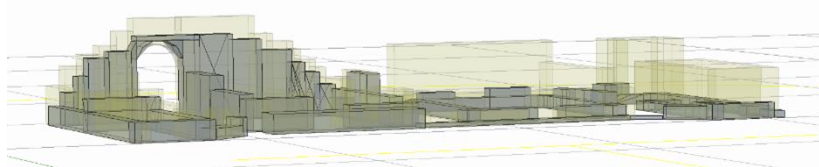


Figure 17: comparison of a detail of the old model (in yellow overlay) and the new one (in gray)

6.2.1 Materials

The new modeling of the theater was also an opportunity to compare the 2015 survey data with the General Plan granted by the Tindari Archaeological Park, and therefore correct some geometric inaccuracies influencing the acoustic behavior and to review the distribution of materials, increasing the level of detail of their mapping. The materials have also been slightly modified in their absorption and scattering coefficients during the numerous calibration tests.

Most of the surfaces of the cavea present a compresence of different material with different physical properties, it is common practice in this case to make weighted average of the absorption coefficients for every octave band, based on the percentage of occupancy of the surface.

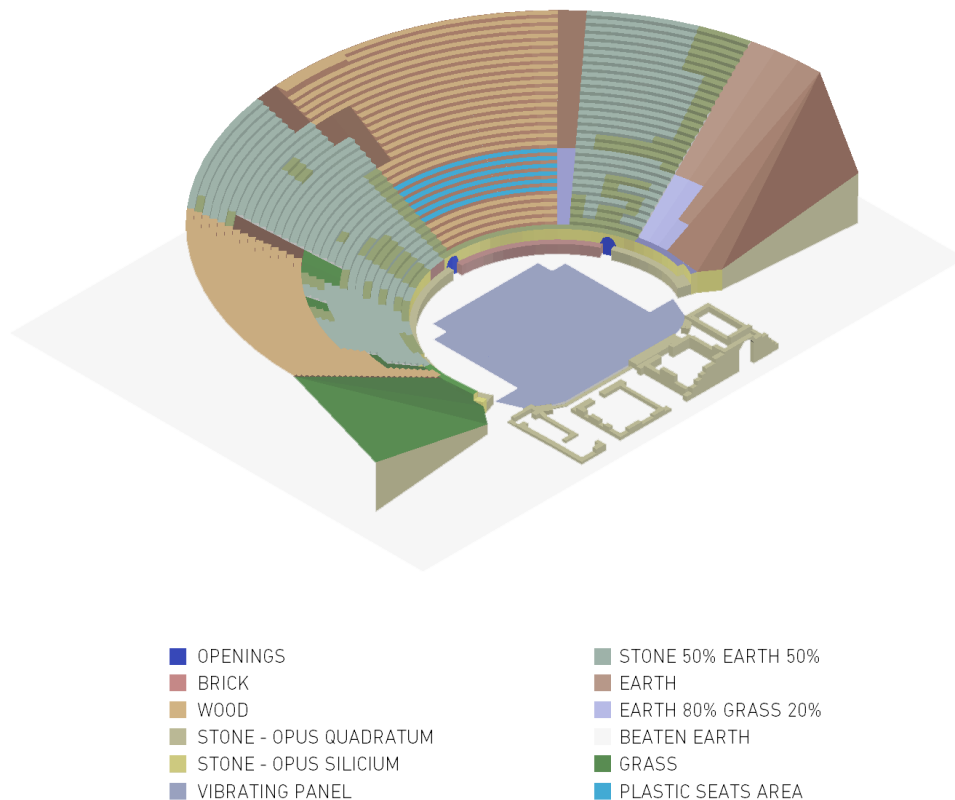


Figura 2: Axonometric view of the model in Autocad showing the distribution of the materials used for the simulations

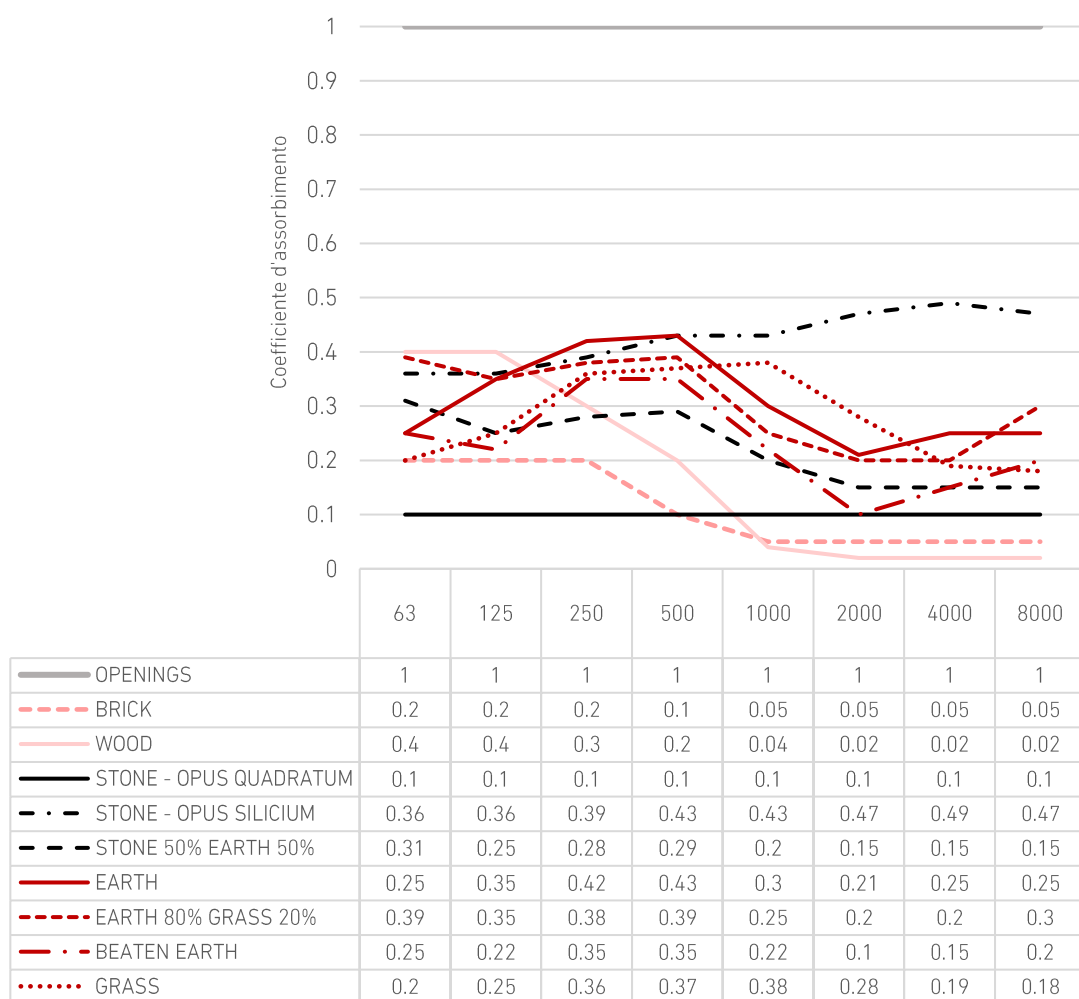


Table 14: axorbtion coefficients for octave bands used for the calibration

Siccome lo scattering non dipende solo dal materiale ma anche dalla geometria e dal grado di scabrezza di ogni singola superficie, si è deciso di assegnare diversi scattering per elementi dello stesso materiale. Un esempio è la parte inferiore del podio composta da pietra arenaria tagliata in grassi blocchi di forma parallelepipedica (opus quadratum) esattamente come i resti della scena; essendo la prima area più uniforme geometricamente e meglio conservata, gli è stato attribuito un coefficiente di scattering del 70%, mentre alla seconda, maggiormente disomogenea e scabra, è stato attribuito uno scattering di 90%.

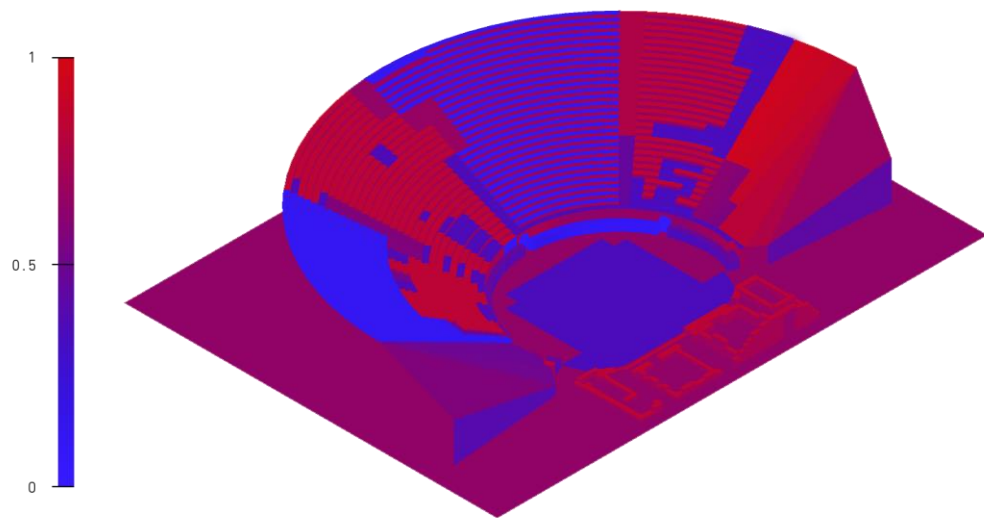


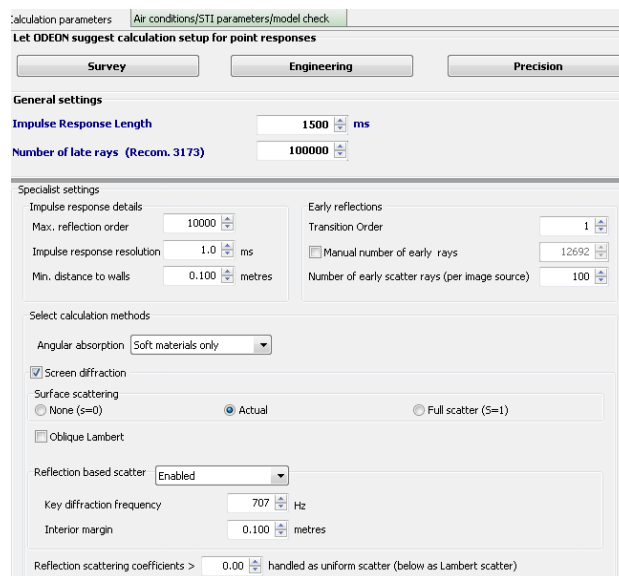
Figure 18: Axonometric view of the model in Autocad showing the the scattering coefficient at 707Hz for every surface of the calibration

Coefficiente di scattering a 707Hz	
OPENINGS	0.01
EARTH	0.8
BRICK	0.5
VIBRATING PANNEL	0.3
STONE - OPUS QUADRATUM	0.7
STONE - OPUS QUADRATUM - SCAENAE	0.9
STONE - OPUS SILICEUM	0.9
WOOD	0.2
PRESERVED TREADS	0.9
EARTH 80 GRASS 20	0.65
BEATEN EARTH	0.8
EARTH 80 STONE 20	0.65
GRASS	0.8

Table 15: scattering coefficients used for the calibration

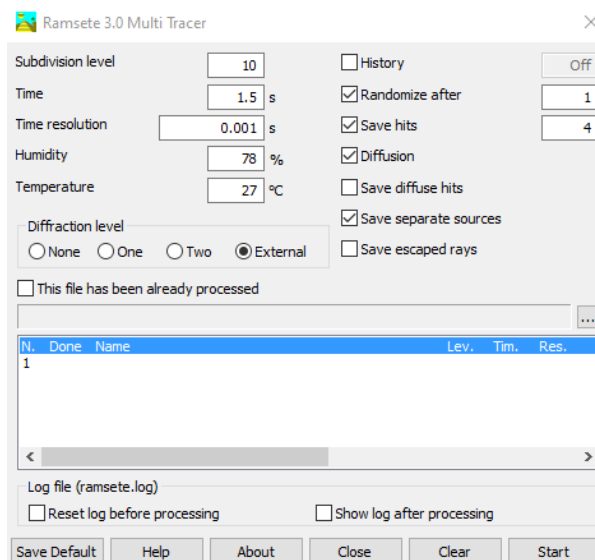
6.2.2 The settings for the simulations

Bellow are reported the settings used for the traicing. The Lambert law for diffusive reflections was disabled because il is batter suited for environments characterized by big, flat, surface, which is not the case for open theaters where the dimensions of the surfaces is often comparable with the wavelength of the signal. For this reason it was prefer the semispherical diffusion algorithm.



The screenshot shows the 'Calculation parameters' dialog box in Odeon. The 'Air conditions/STI parameters/model check' tab is selected. The 'Survey' button is highlighted. The 'General settings' section includes 'Impulse Response Length' set to 1500 ms and 'Number of late rays (Recom. 3173)' set to 100000. The 'Specialist settings' section includes 'Impulse response details' (Max. reflection order: 10000, Impulse response resolution: 1.0 ms, Min. distance to walls: 0.100 metres) and 'Early reflections' (Transition Order: 1, Manual number of early rays: 12692, Number of early scatter rays (per image source): 100). The 'Select calculation methods' section includes 'Angular absorption' (Soft materials only), 'Screen diffraction' (checked), 'Surface scattering' (None (s=0), Actual, Full scatter (S=1)), 'Oblique Lambert' (unchecked), 'Reflection based scatter' (Enabled), 'Key diffraction frequency' (707 Hz), 'Interior margin' (0.100 metres), and 'Reflection scattering coefficients >' (0.00 handled as uniform scatter (below as Lambert scatter)).

Figure 19: Room settings in Odeon



The screenshot shows the 'Ramsete 3.0 Multi Tracer' dialog box. The 'Subdivision level' is set to 10, 'Time' to 1.5 s, 'Time resolution' to 0.001 s, 'Humidity' to 78 %, and 'Temperature' to 27 °C. The 'Diffraction level' is set to External. The 'History' checkbox is unchecked, and 'Randomize after' is checked with a value of 1. 'Save hits' is checked with a value of 4. 'Diffusion' is checked. 'Save diffuse hits' is unchecked. 'Save separate sources' is checked. 'Save escaped rays' is unchecked. The 'This file has been already processed' checkbox is unchecked. The 'Log file (ramsete.log)' section includes 'Reset log before processing' (unchecked) and 'Show log after processing' (unchecked). The 'Save Default', 'Help', 'About', 'Close', 'Clear', and 'Start' buttons are at the bottom.

Figure 20: settings for Ramsete Tracer

6.3 Results of the calibration

The parameters considered for the calibration are the same used for the previous one in 2020, i.e. the T20 and G. They have been compared to the corresponding results of the analysis of the IRs obtained during the measurement campaign of 2015. The reference values are an average of the results obtained with the three types of sources (the firecrackers “Raudo Manna New Ma1b” and “Perfetto C00015 Raudo New”, and the dodecaedron “Bruel & Kjaer Omnipower sound source 4296”), calculated for each octave band from 125 Hz to 8 kHz.

The MAD method verifies the T20 and G for both the calibrations in Odeon and in Ramsete, with differences that don't surpass the threshold of the JND as defined in ISO 3382-1: 2009, i.e. 5% for T20 and 1 dB for G. Nevertheless the differences between the two simulations are very noticeable in graphics show in the following pages, especially in the diagram of T20, where the curve of the simulation in Odeon appears to be very similar to the one obtained in the simulation of 2020, and it is not contained in the range of the JND on the octave bands of 125 Hz, 250 Hz, 2000 Hz and 8000 Hz.

The T20 calculated in Ramsete is instead almost identical to reference, and it surpasses the JND only on the 125 Hz octave band.

The diagram of G_{mid} shows the values of the robustness index for every receiver (represented by a circle, a cross or a square) in relation to its distance from the source, and the relative trendline for three simulations. The trendlines of the values of the survey and the curve of the free field hypothesis are also shown as a reference. It is noticeable how the robustness of the Ramsete model is more or less 0.5 dB higher than the two Odeon model, the average value of G for Odeon is in fact -4.2375, against the -2.725 of Ramsete.

Although the results of T20 and G of the Odeon model resemble the ones obtained by G. Benvenuto in her previous simulation, the parameters of C50 presents some differences at lower frequencies, the largest of which is the -1.8 dB at 250 Hz.

The deviation observed for the T20 at 125 Hz could be caused by the poor reliability of the measurements on that frequency band, due to a bad INR (impulse to noise ratio), as previously mentioned during the analysis of the simulations of 2020. For this reason, the results of the calibration have been considered acceptable to prosecute to the next phase of the work.

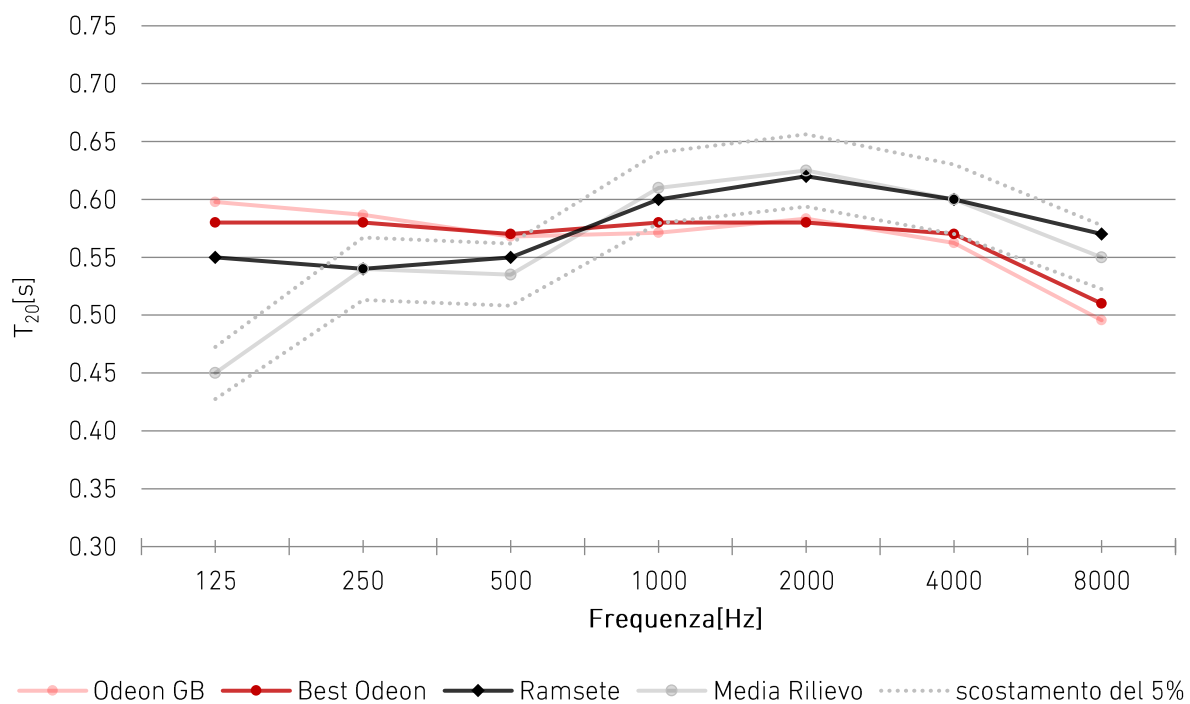


Table 16: T20 acoustical models results compared with the results of the survey

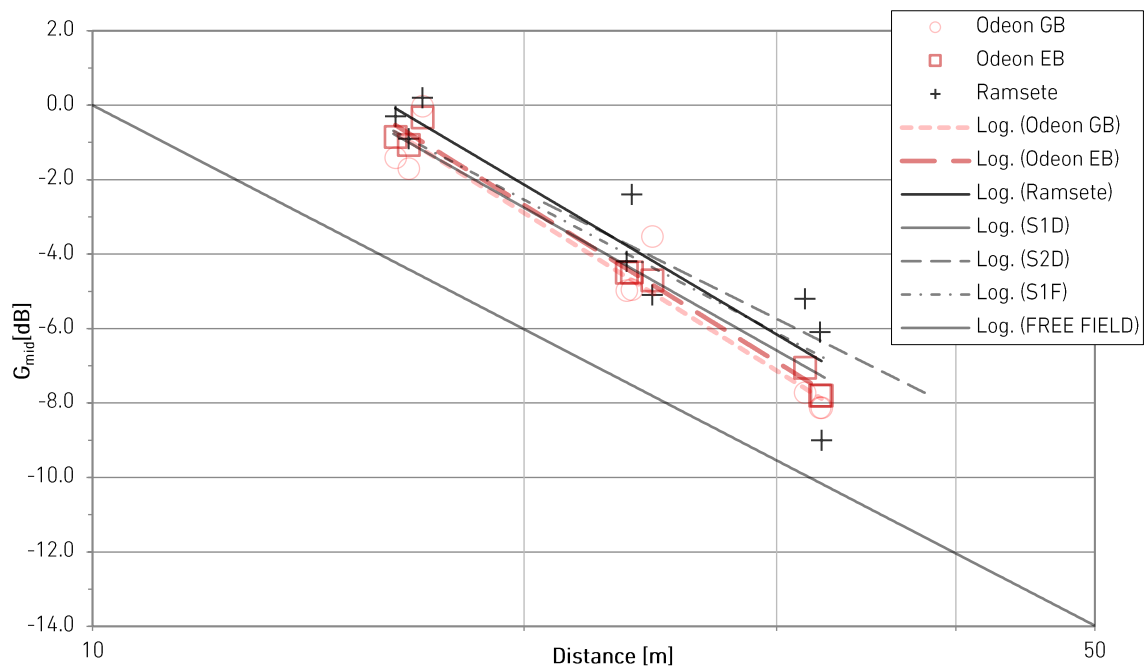


Table 17: Confronto tra valori di G medi misurati e simulati per tutti i ricevitori in base alla distanza.

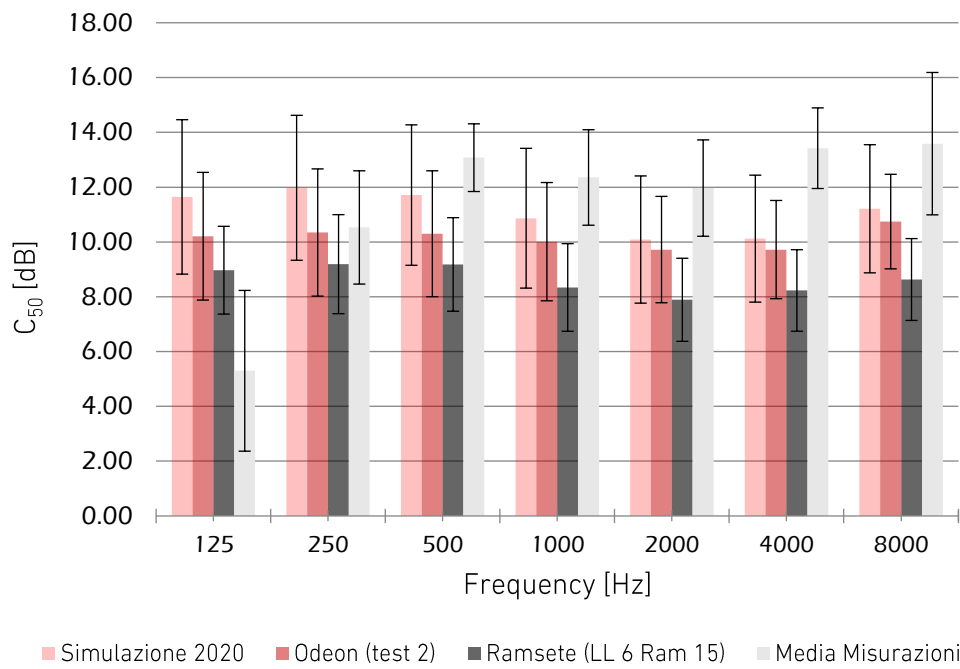


Table 18: C_{50} of the calibration model, for all the receivers and sources, expressed as a function of frequency. Standard deviations are reported on the error bars.

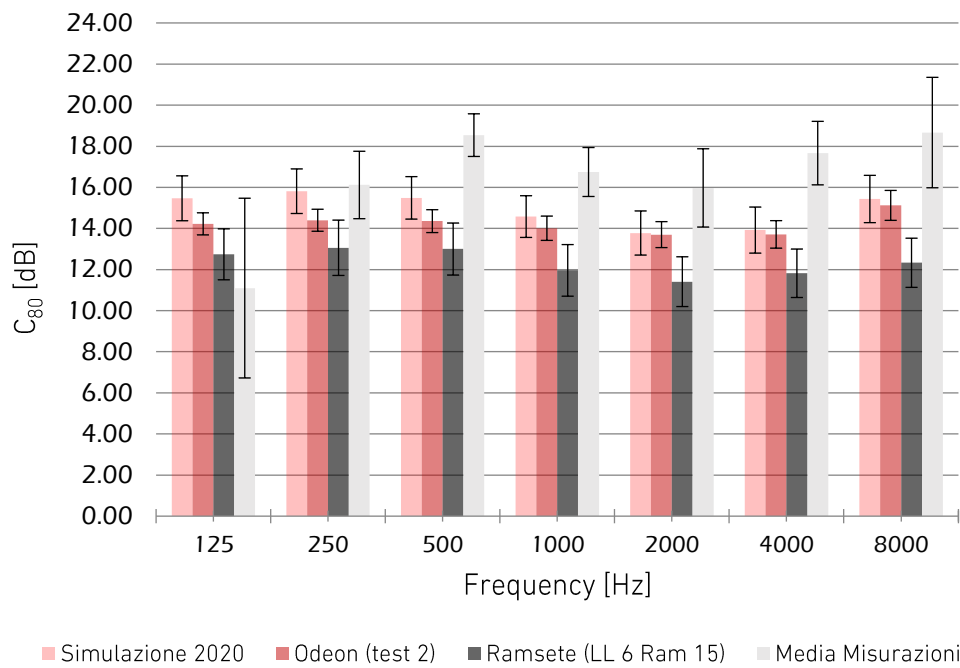


Table 19: C_{80} of the calibration model, for all the receivers and sources, expressed as a function of frequency. Standard deviations are reported on the error bars.

6.4 Reconstruction of the past

The models of the Greek and Hellenistic configuration maintain the same settings and the same coordinates of Source and Receivers used for the calibration. The original shape of the cavea and the scaenae frons has been reconstructed following the description written by Bernabò Brea, director of the of the restauration works of 1960, in his “Due secoli di studi, scavi e restauri del teatro greco di Tindari” (Bernabò Brea, L. 1964-1965).

The cavea has been taken back to the original, perfectly circular, shape that it presented before been altered by the gradual sliding of the soil. The original perimeter of the orchestra was determined following Bernabò Brea’s guidelines: “The fronts of the koilon's wings were not straight, but broken off at an obtuse angle having the vertex almost exactly half of their length. That is, they began to the external angles of the koilon on the same line corresponding to a chord that cut the radius of the orchestra about two thirds of its length. If they had continued on this line they would have reached almost exactly the front of the paraskenia and there would have been no parodoi.

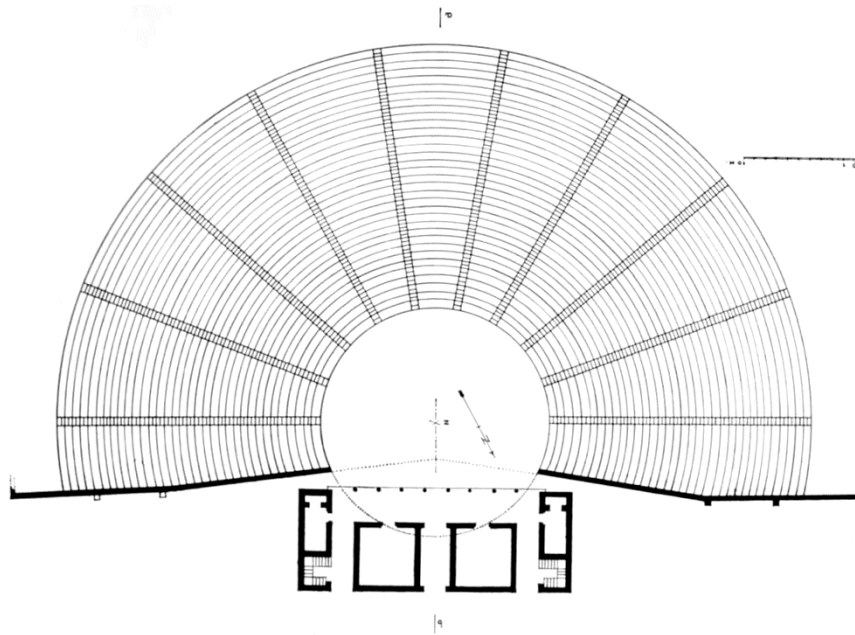


Figure 21: Reconstruction of the Plan of in the Hellenistic period (Bernabò Brea, L. 1964-1965)

In order to obtain the parodoi, it was therefore necessary to interrupt this initial trend of the fronts of the koilon's wings and give them a direction converging towards a point moved towards the center of the orchestra by another third of the radius. This way they obtained the parodoi of m 1.10 of width, just enough to allow the access of the spectators to the orchestra.”

Four steps has been added to account for the ones removed by the Romans to build the podium. Bernabò Brea hypothesized six more on around the summa cavea, but he also states that it not clear if that space was occupied by an ambulacro or diàzoma, so they were not taken into account for this reconstruction.

The only difference between the Greek configuration and the Hellenistic is the presence of the scaenae frons in the second one.

The model of the scene follows the graphic reconstructions developed by H.Bulle after a careful analysis for the blocks unearthed by the excavations of 1845 and later perfected by Bernabò Brea.

Two different LOD of details have been chosen: low level of detail for the acoustic model, and high detail for the VR model.

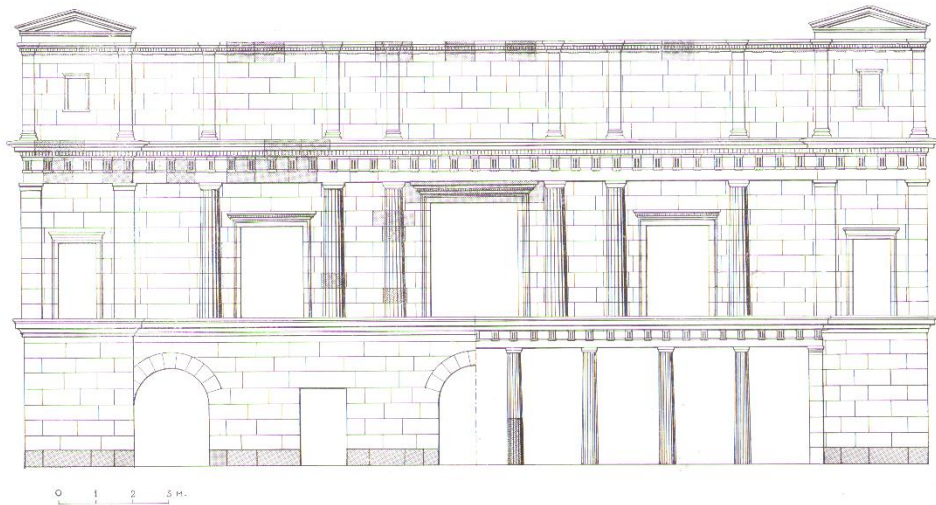


Figure 22: Graphic reconstruction of the scaenae frons (Bernabò Brea, L. 1964-1965)

The materials used for this simulation are taken directly from the calibration model and reordered to try match, as accurately as possible, the original position of every element and its original absorption and scattering coefficient, altered in time by deterioration.

The cavea has been assigned two materials: highly reflective stone (the same used for the podium and scaenae frons of the calibration model) for the rise

of the steps, and a mix of stone and earth for the tread made by averaging the absorption coefficients of these two materials.

The simplification of the geometry of the scaenae frons has been counterbalanced by a high scattering coefficient (0.9 at 707Hz). The scene was in fact originally designed to be highly diffusive in order to avoid echoes.

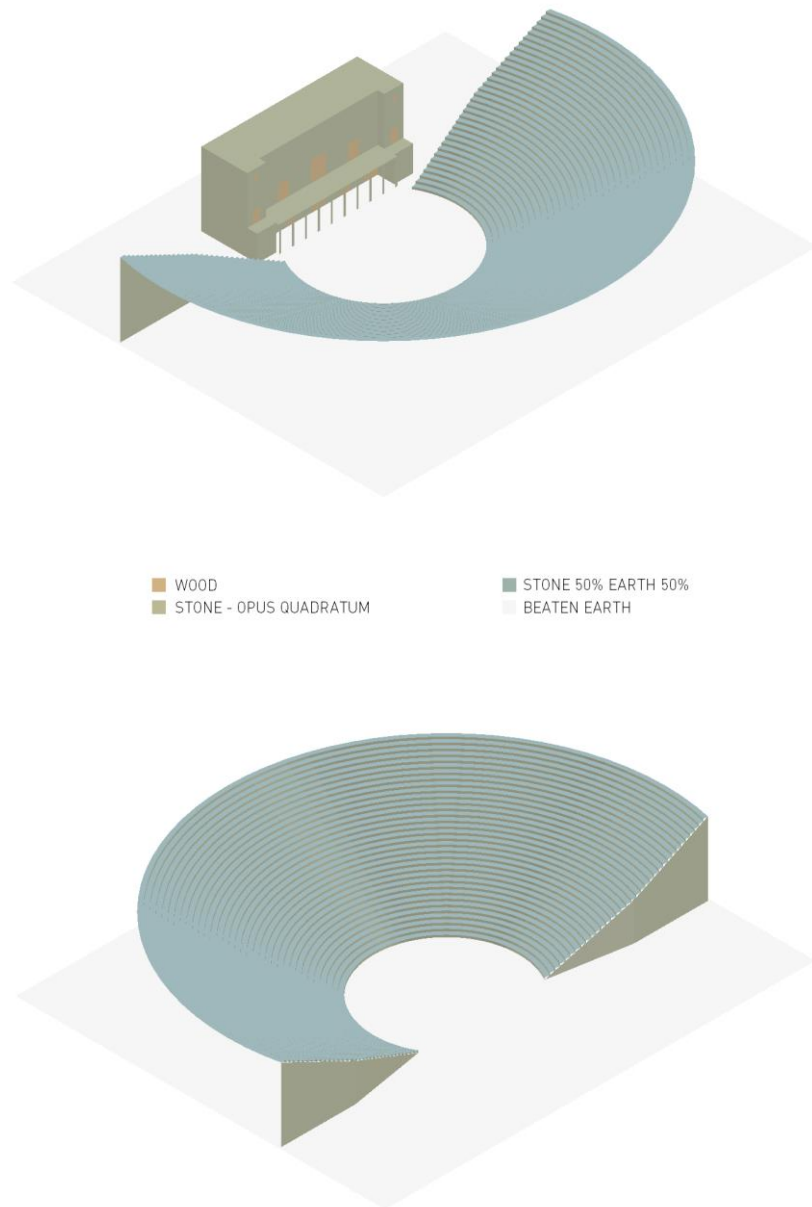


Figure 23: Axonometric view of models used for the Hellenistic simulation (above) and for the original Greek configuration. The properties of the materials illustrated are the used for the same material in the calibration model.

6.4.1 Results of the simulation of the Hellenistic configuration

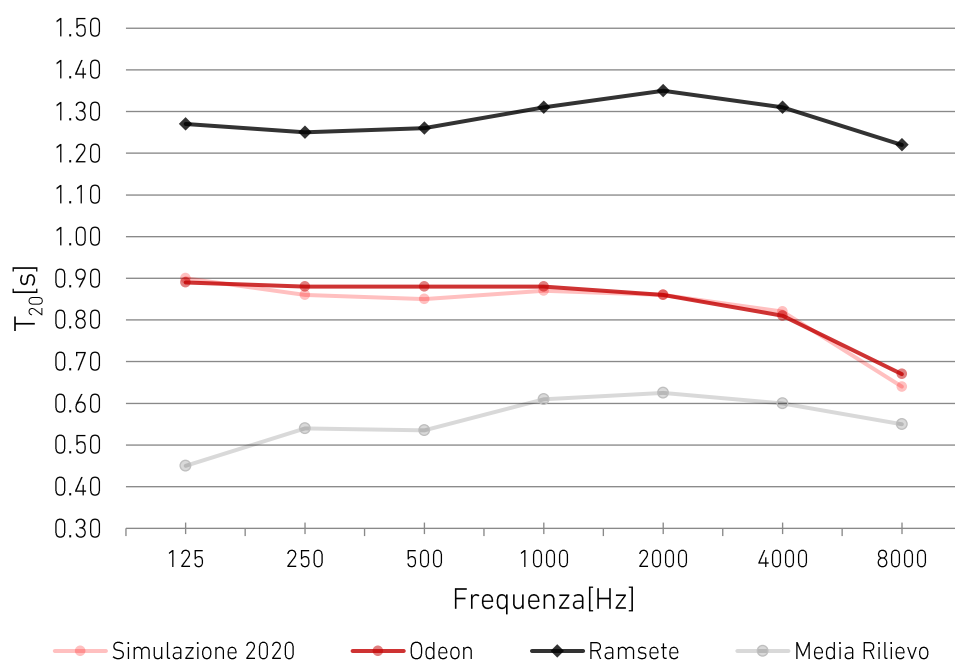


Table 20: T_{20} of the Hellenistic acoustical models compared to the results of the survey of 2015.

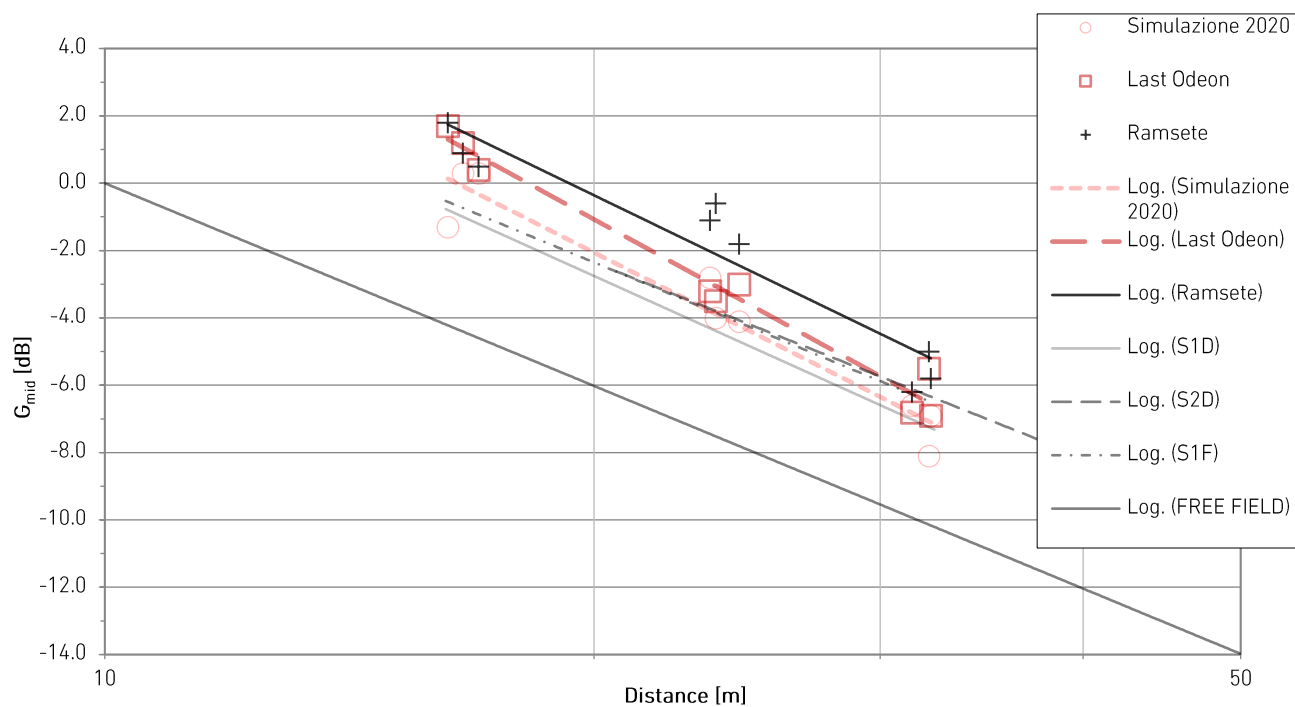


Table 21: G_{mid} of the Hellenistic acoustical model for every receiver compared to the results of the survey of 2015.

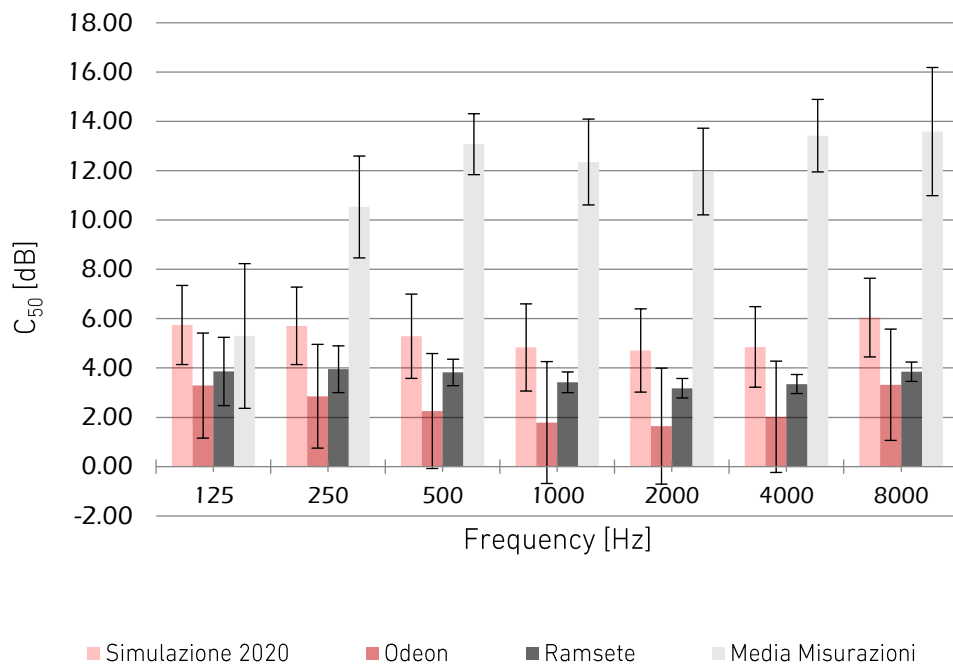


Table 22: C_{50} of the Hellenistic acoustical model, for all the receivers and sources, expressed as a function of frequency. Standard deviations are reported on the error bars.

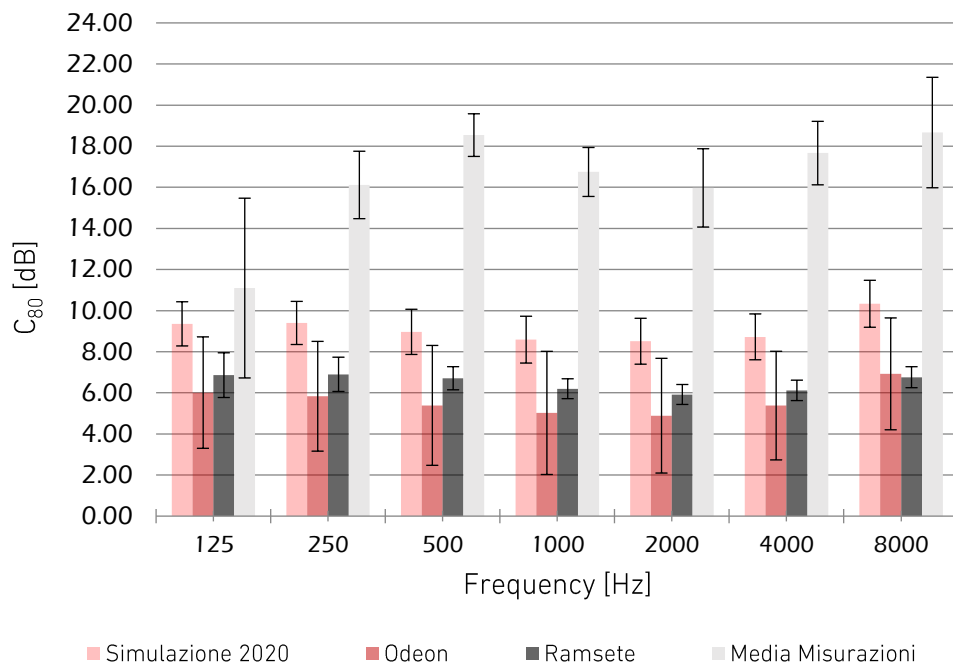


Table 23: C_{80} of the Hellenistic acoustical model, for all the receivers and sources, expressed as a function of frequency. Standard deviations are reported on the error bars.

6.4.2 Results of the simulation of the Greek configuration

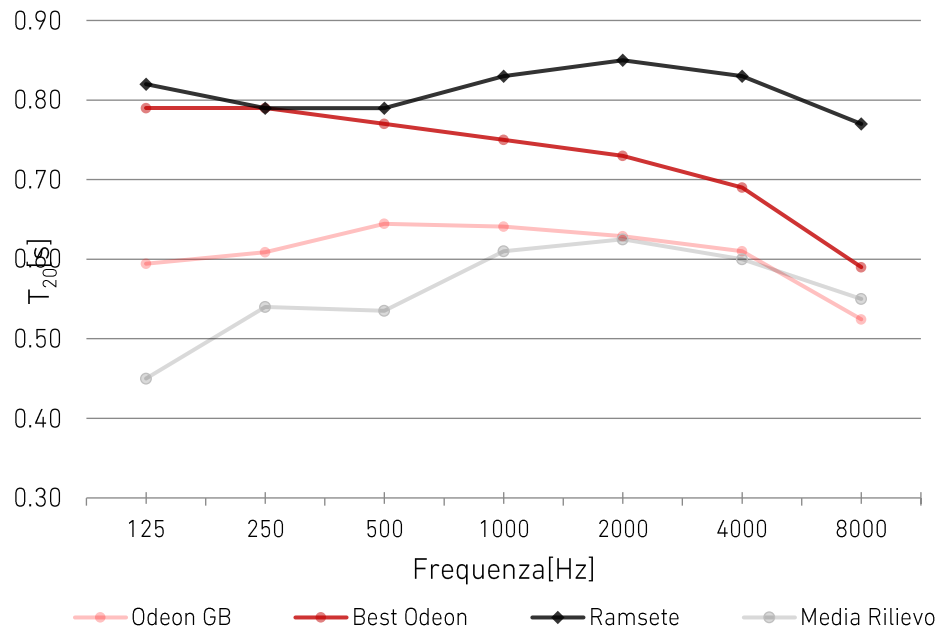


Table 24: T_{20} of the Greek acoustical models compared to the results of the survey of 2015.

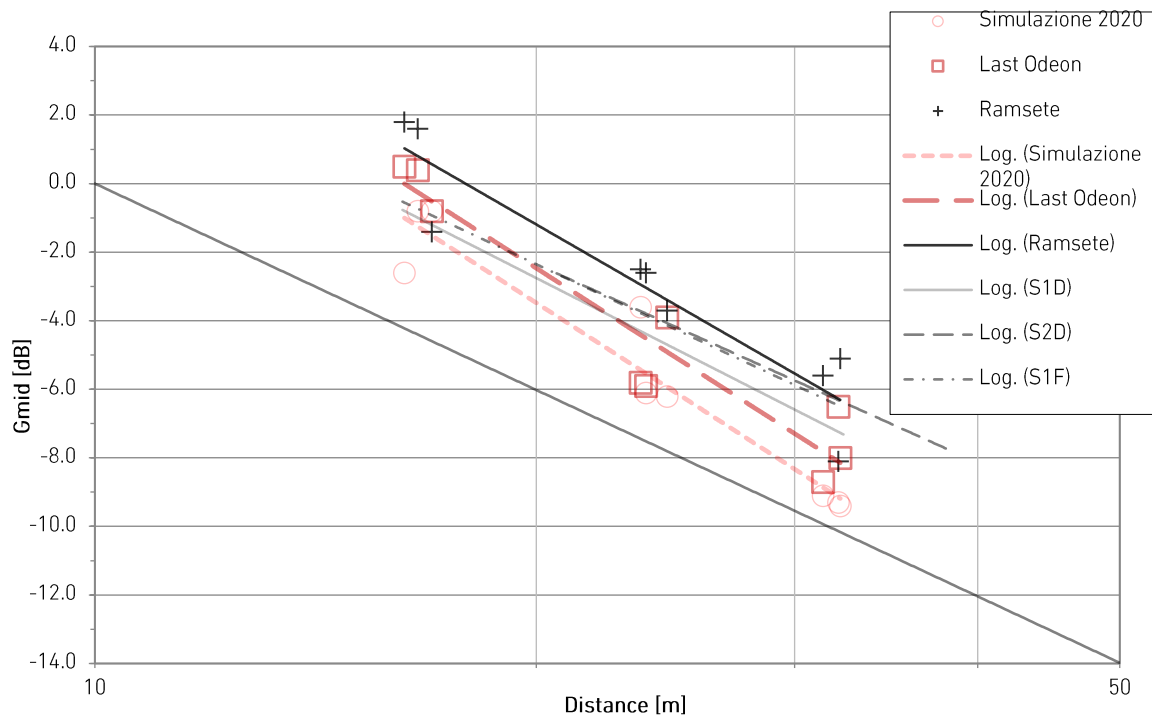


Table 25: G_{mid} of the Greek acoustical model for every receiver compared to the results of the survey of 2015.

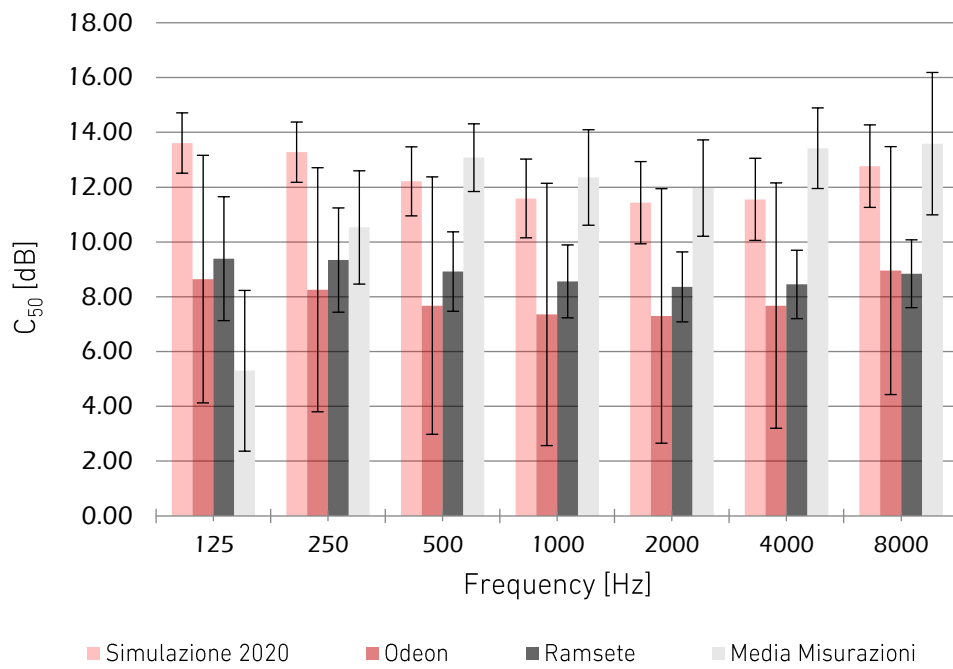


Table 26: C_{50} of the Greek acoustical model, for all the receivers and sources, expressed as a function of frequency. Standard deviations are reported on the error bars.

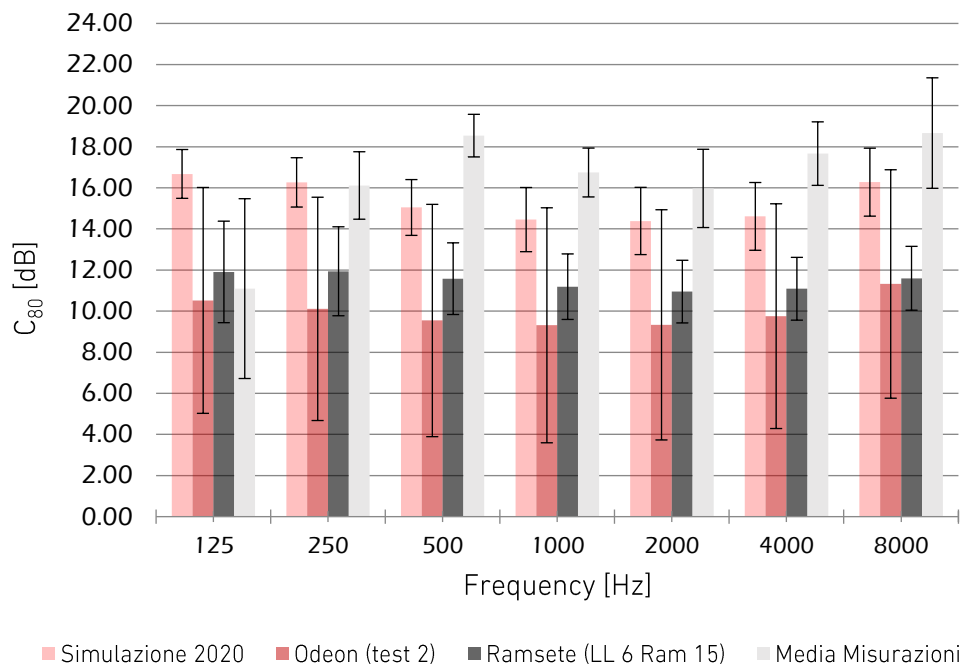


Table 27: C_{80} of the Greek acoustical model, for all the receivers and sources, expressed as a function of frequency. Standard deviations are reported on the error bars.

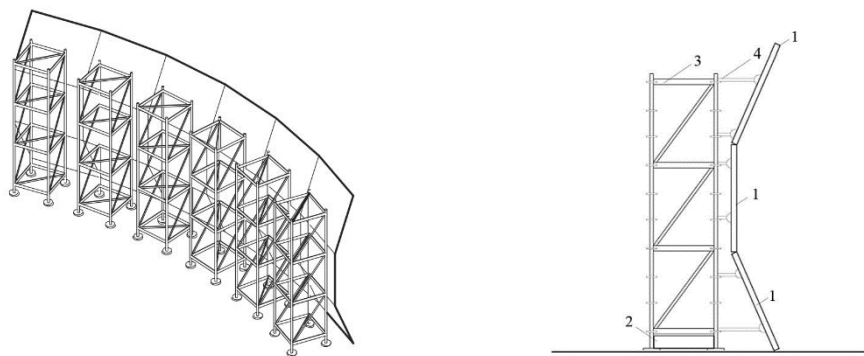
6.5 Proposed future configuration

The Syracuse Charter for the conservation, fruition and management of ancient theatrical architecture explains the the risks and the inevitable deterioration caused by public fruition, but also highlights the how the incrementation of their performances and the direct experience from wide audience permits to extend the knowledge of their intrinsic value ('Carta di Siracusa "per la conservazione, fruizione e gestione delle architetture teatrali antiche"', 2014).

In 2016 Giovanni Bouvet proposed an optimization of the acoustics of the theatre in its current state of deterioration state by designing a new scene that took advantage of the Canac Laws to create early reflections that can contribute to the perceived loudness of the signal.

The curved shape of the reflector was generated by an evolutionary solver, Galapagos, a plugin for Grasshopper² deploying computational morphogenesis, using a simple ISM (Image Source Method) algorithm, partially based on François Canac's studies.

The structure was designed taking into account recommendations of the Syracuse Charter, asserting that temporary structures can integrate the gaps in order to optimise the acoustic performance: the modular modular approach allows for a lightweight removable structure, illustrated bellow, that doesn't impose any permanent impact on the archeological site (Bouvet et al., 2020).



- 1. MDF panel - 19 mm depth
- 2. Ballast
- 3. Supporting reticular structure
- 4. Telescopic joint with adjustable head

Figure 24: Hypothetical structural solution for the designing of the shell.
Image courtesy of Giovanni Bouvet

² Grasshopper is a popular node-programming environment that allows for procedural modelling Rhinoceros 3D

By inserting this new new element in the updated simulation of the current state of the theater we can further evaluate how it can impact the acoustic performance not only through the comparison of the acoustic parameters, but also through the direct sensorial experience made possible by the auralization process.

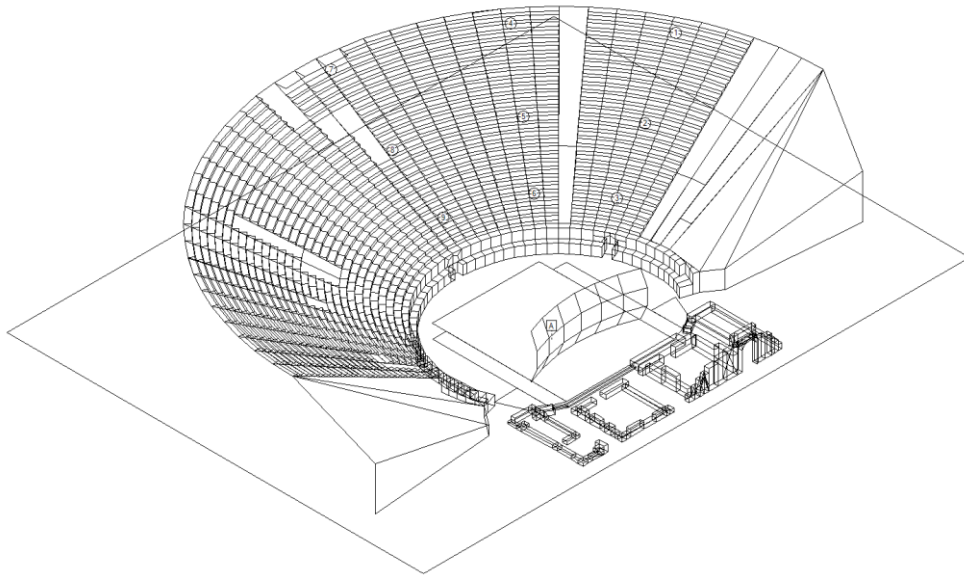


Figure 25: A isometric view in Ramsete

The simulation of the current state was then repeated after importing the additional shell and assigning an absorption coefficient of 0.05 on the whole spectrum to the highly reflective MDF panels, and a scattering coefficient of 0.2 for 707Hz.

The material for the orchestra shells' panels has to be highly reflective, so the choice fell on Medium Density Fibreboard, MDF, which is a light and resistant wooden material characterized by $\rho = 800 \text{ kg/m}^3$, and $\alpha_w = 0.05$, constant for frequency from 500 Hz to 8 kHz.

The results of the simulation are illustrated below in the next pages.

As expected, the Robust Index increase noticeably both in Ramsete and in Odeon. The C50 is also higher, which translates in a better listening experience for the spoken word, and a lower strain for the speaker in the orchestra to be heard.

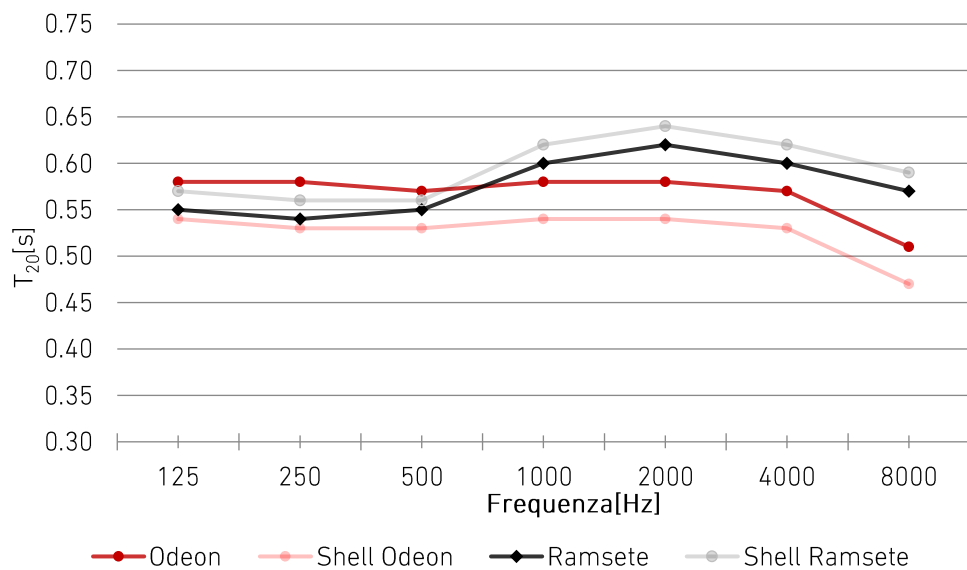


Table 28: T20 of the current state optimized with the reflective Shell.

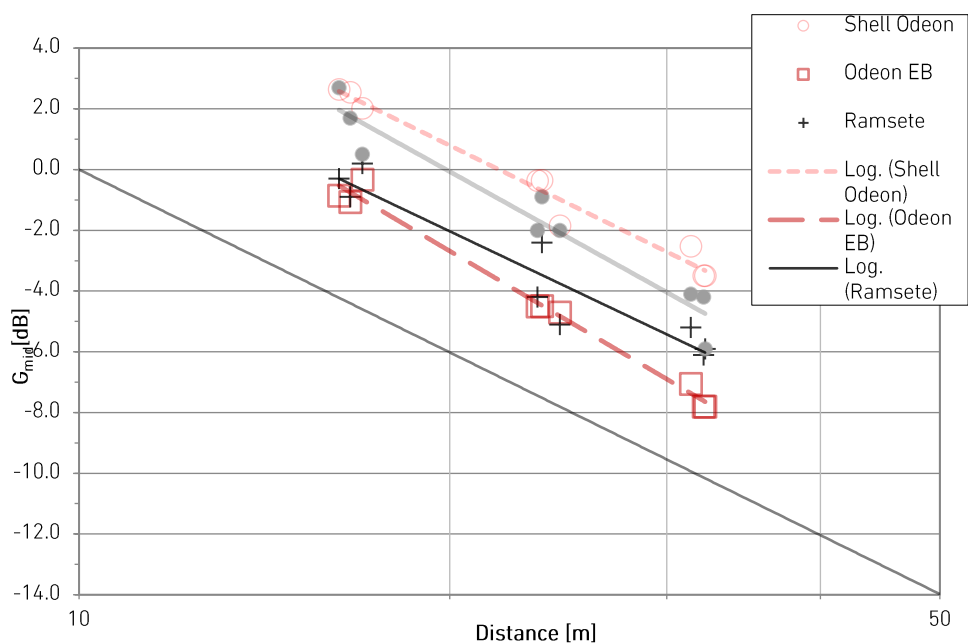


Table 29: G_{mid} of the current state optimized with the reflective Shell.

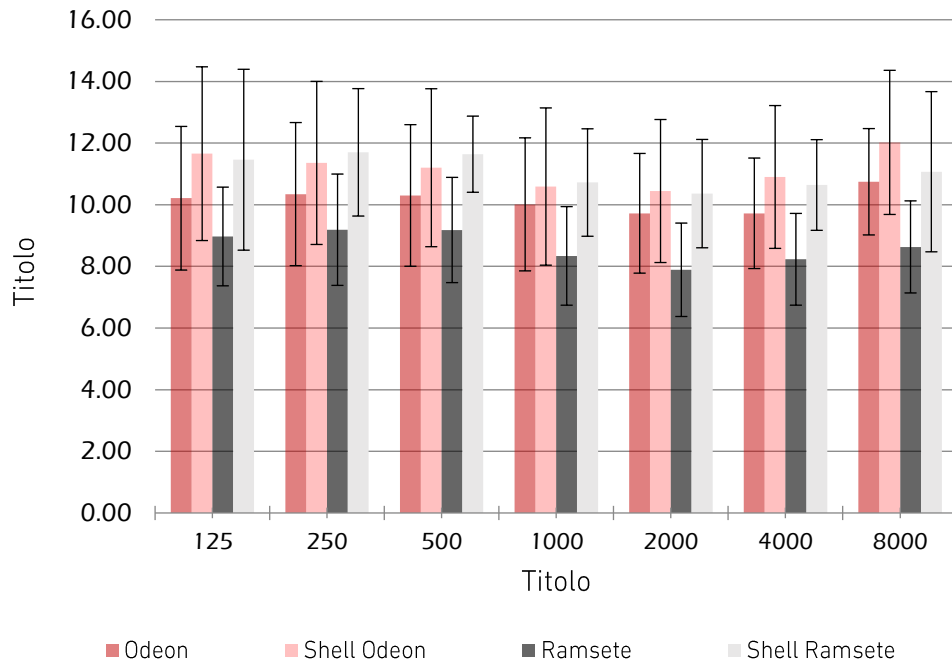


Table 30: C_{50} of the current state optimized with the reflective Shell, for all the receivers and sources, expressed as a function of frequency. Standard deviations are reported on the error bars.

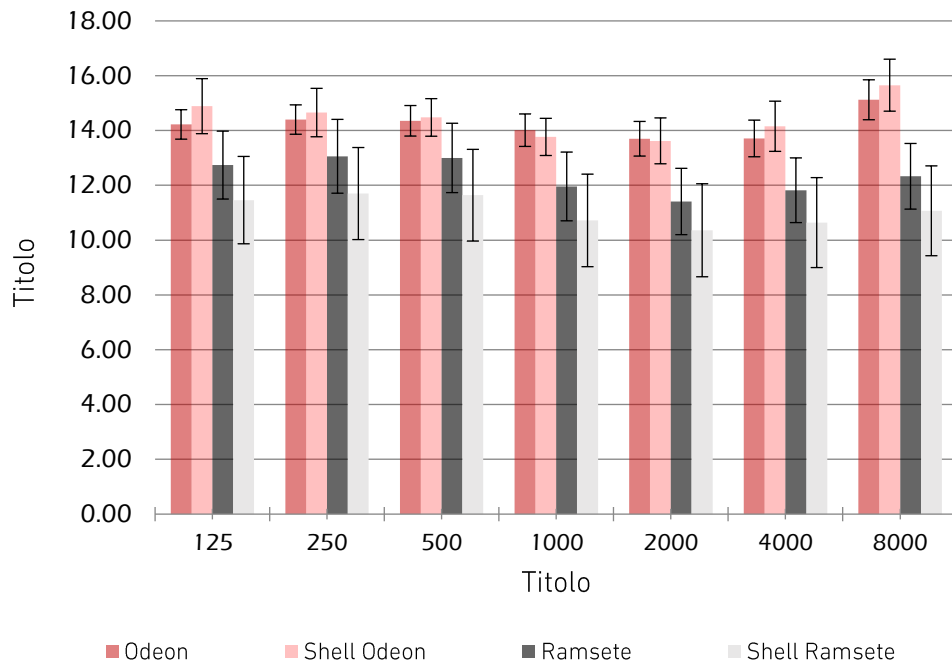


Table 31: C_{80} of the current state optimized with the reflective Shell, for all the receivers and sources, expressed as a function of frequency. Standard deviations are reported on the error bars..

6.6 Comparison between the configurations

The reintegration of the missing parts of the cavea, together with the virtual reconstruction of the frons scenae, together with the generated, as expected, a noticeable increase of the T20 and G, what is surprising is the drastic decrease of C50 and C80. Longer reverberation times are usually accompanied by a decrease in clarity, but since the ancient open theatres were designed to facilitate the vocal communication, the C50 registered for the Greek and Hellenistic configurations is suspiciously low and will need further evaluations. Echoes effects were registered in the Impulse Responses of these simulation, although the scattering coefficient applied to the surfaces was very high.

On that regard, the performance of the reflective shell proves the effectiveness of the project of Giovanni Bouvet, and is encouraging in the perspective of a recovery of the original sound quality of ancient open theatres.

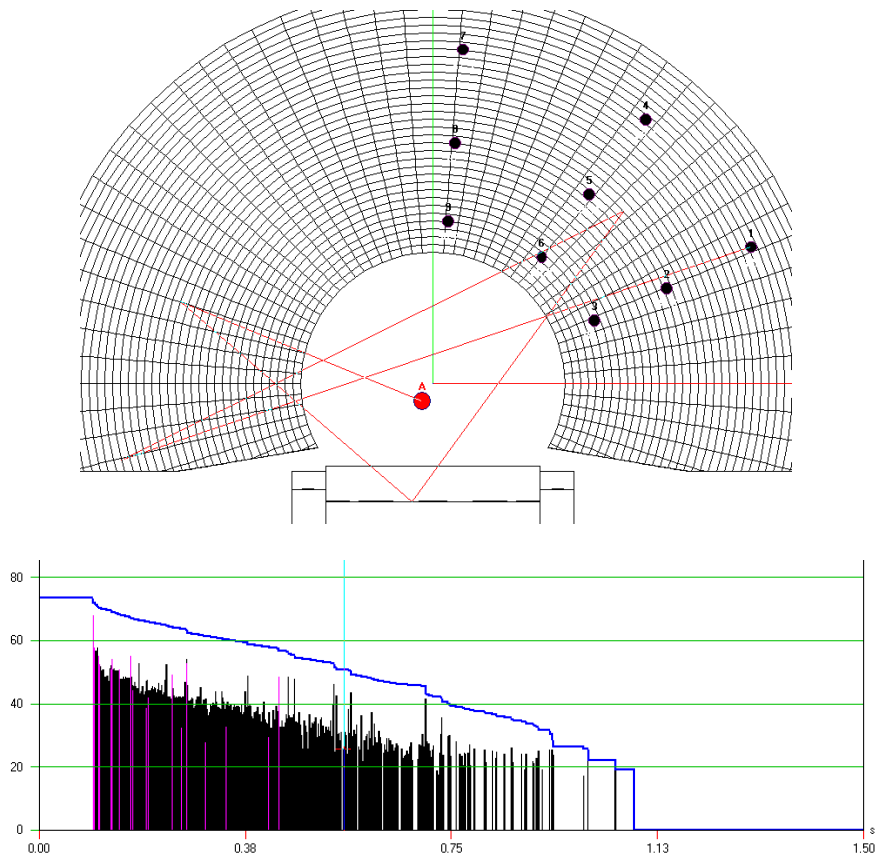


Figure 26: an example of disturbing late reflection traced in Ramsete

7. AURALIZATION AND VIRTUAL REALITY

7.1 Auralization

The Impulse Responses synthesized with Odeon and Ramsete can be exported in B-Format used to convolute anechoic samples of speech or music. The auralization in this format offer a much more versatility than the old method of binaural convolution, which is restricted to the use of headphones and requires a personalized Head Related Transfer Function (HRTF).

Ambisonic auralization can be played both by speakers, if properly set up, and by headphones provided with rotational tracking. Nowadays this kind of headphones are becoming more and more common because they are implemented in any HMD (Head Mounted Display) such as the widespread Oculus Quest.

However, the main advantage of the ambisonic playback is the possibility of rotating one's head without "rotating the hole soundfield", this is valid both for speaker arrays then tracked headphones.

This chapter will describe the workflow developed to use of the IR obtained with the simulations of the previous chapter to create an immersive audio-visual experience of the theatre of Tindari in of its previously described configurations.

All the software used in this chain are open source or free to use.

Specifically they are: Audacity , Aurora, Blender, FFmpeg, Spatial Media Metadata Injector, and Vlc, for the production part.

The following Vst (Virtual Studio Technology) where used for the analytic part: Sparta | PowerMap, Sparta | DirASS and O3A Flare.

7.2 The visual component

The original plan for this project contemplated a new field mission to Tindari, to conduct acoustic surveys with the a MIMO (Multiple Input Multiple Output) probe and to perform a photogrammetric scan of the building with drones.

This would have made it possible to create a highly realistic model that favors the immersive experience, but having been postponed to campaign to spring of 2022, the reconstruction was created from scratch with the Blender. It consists of nine equirectangular panoramic images for each of the configurations of the theatre, each associated with a Receiver point and its corresponding High Order Ambisonics impulse response. Some views of the resulting 3d models are shown at the end of the chapter.

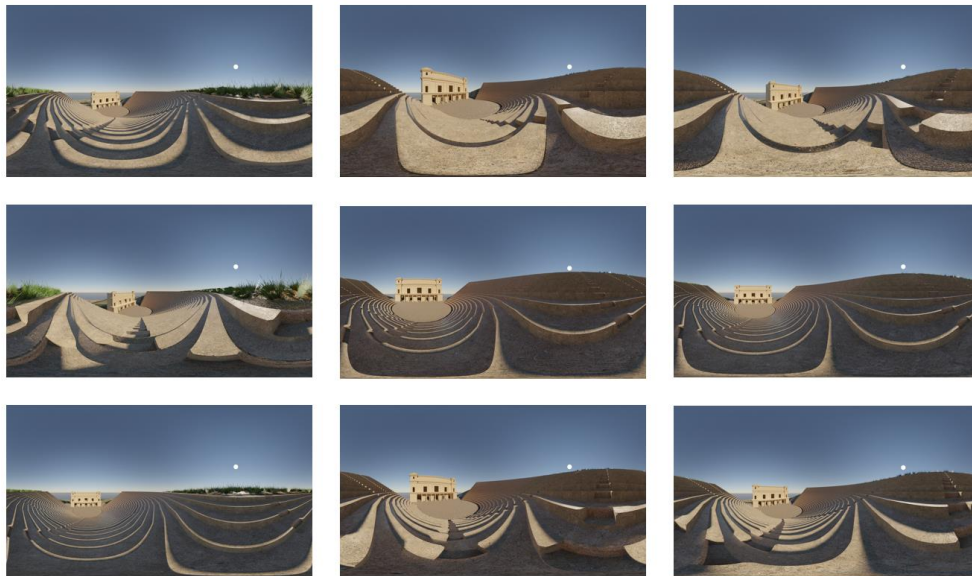


Figure 27: Equirectangular Renderings from the points of view of the 9 receivers in the cavea

7.3 The audio component

Odeon contains a very practical tool to produce auralizations, but, for it was instead preferred to create the auralizations of its IRs with the same convolver used for IRs coming from Ramsete, specifically the free plugin *Aurora* for Audacity, developed by professor Angelo Farina.

The choice of the sample to use for the convolution is not trivial when the objective is to create an immersive experience: any sample that can be perceived as “out of context” in ancient Greek theatre has to be discarded.

The optimal solution would be to convolve an anechoic sample of the enactment of ancient Greek plays or music.

Historian and musicologists, as professor Armand D'Angour from Oxford University, are developing these kind of faithful reconstructions, but no proper studio recording is available yet, so the default samples of Odeon's anechoic sound library were used instead. Prof. D'Angour kindly offered me

the recordings of his reconstructions of songs written by the Athenian tragedian Euripides for the choir of Orestes in 408BC. This would have been a perfect sample if it wasn't for the strong reverberation of the room it was recorded in, which would invalidate the truthfulness of the auralization. The sample rates of the IRs were then matched with those of the anechoic files, and the samples were convolved to AO 1, 2, 3, 4 and 5. The audio was then analyzed to check the orientation of the sound field and to evaluate its quality. This was done in the in Reaper, a powerful, free to use Digital Audio Workstation that natively supports ambisonics, with PowerMap, Sparta | DirASS and O3A Flare, VSTs that permit the visualization of the energy levels in the sound field.

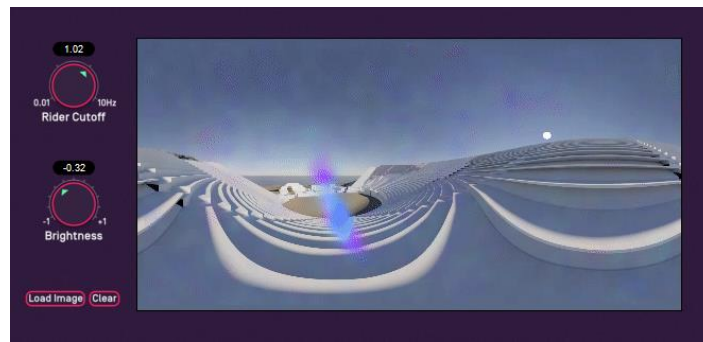


Figure 28: The Vst O3A Flare showing the precise location of the sound source in a 5thOA Impulse Response.

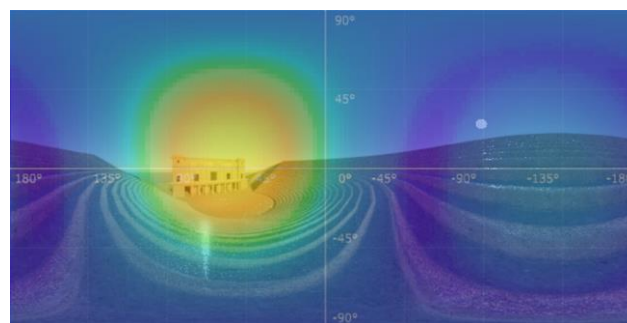


Figure 29: The Vst Sparta | PowerMap showing a somewhat blurred localization of the soundsources in a 1stOA impulse response.

7.4 La creazione dei video in VR

The final stage was multiplexing, that is the merging of the audio and video components.

The quadrirectangular images where converted to videos with FFmpeg using the following command:

```
.\\ffmpeg -loop 1 -i 1.png -c:v libx264 -t 22 -pix_fmt yuv420p Video-01.mp4
```

Audio and video where then muxed with the command:

```
.\\ffmpeg -i Video-01.mp4 -i ConvBFormatAural01.Wav -map 0:v -map 1:a -c:v copy -c:a copy -shortest 1.mov
```

The result is a .mov file that can be transformed into a 360-degree video by injecting the appropriate metadata with Spatial Media Metadata Injector, a software developed by Google and modified by Angelo Farina to extend its usability for HOA (Higher Order Ambisonics).

They can be watched on Vlc, on any HMD, and the videos of the first order of ambisonics can be watched on Youtube, as 360 videos with rotation tracking, at the link contained in the following QR code:





Figure 30: Render of the 3d of the current state with the addition of the reflective acoustic shell designed by G.Bouvet



Figure 31: Render of the 3d of the current state with the addition of the reflective acoustic shell designed by G.Bouvet



Figure 32: Render of the 3d reconstruction of the Hellenistic configuration

8. CONCLUSIONS

Three comparisons were at the center of this thesis, their results can be briefly summarized as follows:

1. The *comparison between Odeon and Ramsete* revealed that even if the calibration models had similar results, the reconstruction models presented a large discrepancy between the values of T20, G, C50 and C80 of the two models. Considering this we can't confirm their accuracy of neither of the two versions of the reconstructive models. More studies and more round-robin tests are needed in order to reach results that can hold an historical value.
2. The *comparison between the different configurations* demonstrated that the difference between the current deterioration state of the theatre and its previous Greek and Hellenistic configurations is very noticeable to human ear and that the original acoustical performance of the theatre is partially recoverable with nonintrusive and sustainable solutions through the implementation. Generative modelling was proved to be very effective in tackling the low Robustness of the soundfield of the theatre.
3. The *comparison between orders of Ambisonic* revealed that the localization of the direction of the source and also the direction of the echoes is more and more precise increasing the AO from 1 to 3, both for the subjective perception of the author and the soundfield analyzers previously mentioned. Although the first order provides less detail it presents the advantage of being supported by internet platforms, it is then the most useful for sharing knowledge with a wide public. It's worth considering to conduct some ABX test to evaluate empirically which of the VR simulations developed provide a better localization of the sound images.

9. REFERENCES

- Astolfi, A. *et al.* (2020) ‘Measurements of Acoustical Parameters in the Ancient Open-Air Theatre of Tyndaris (Sicily, Italy)’, *Applied Sciences*, 10, p. 5680. doi:10.3390/app10165680.
- Beatthezombie (2021) *Spherical Harmonic Basis Functions*, *Computer Graphics, Software Development and Math*. Available at: https://beatthezombie.github.io/sh_post_1/ (Accessed: 22 November 2021).
- Benvenuto, G. (2020) *Il teatro antico di Tindari: ricostruzione virtuale dell’evoluzione acustica*. Tesi Magistrale. Politecnico di Torino.
- Bernabö Brea, L. (1965) *Due secoli di studi, scavi e restauri del teatro greco di Tindari*.
- Binelli, M., Pinardi, D. and Farina, A. (2018) *Individualized HRTF for playing VR videos with Ambisonics spatial audio on HMDs*.
- Bo, E. (2017) *Archaeoacoustics, from antiquity to nowadays Contemporary use of the classical ancient architecture for performing arts*. Doctoral Dissertation. Politecnico di Torino.
- Bouvet, G.A. *et al.* (2020) ‘Computational design: acoustic shells for ancient theatres’, in *Forum Acusticum*. Lyon, France, pp. 1581–1585. doi:10.48465/fa.2020.0838.
- ‘Carta di Siracusa “per la conservazione, fruizione e gestione delle architetture teatrali antiche”’ (2014).
- Christensen, C.L., Koutsouris, G. and Gil, J. (2020) ‘ODEON Room Acoustics Software’, p. 259.
- Cole, J. (2007) ‘Music and Architecture: Confronting the Boundaries between Space and Sound Transcript’, in.
- Farina, A. (1995) ‘RAMSETE-a new Pyramid Tracer for medium and large scale acoustic problems’.

Farina, A. (2017) *HOA Explicit Formulas*. Available at: http://pcfarina.eng.unipr.it/Aurora/HOA_explicit_formulas.htm (Accessed: 21 November 2021).

Farina, A. (no date) *How to create a 360-video for Youtube with both an Ambix 'SPATIAL AUDIO' track plus an 'head-locked' stereo track*. Available at: <http://pcfarina.eng.unipr.it/Ambix+HL.htm> (Accessed: 21 November 2021).

Farina, A., Galaverna, P. and Giabbani, M. (1998) 'IL PROCESSO DI AURALIZZAZIONE: METODOLOGIA ED ESEMPLIFICAZIONE'.

Funkhouser, T. et al. (1998) 'A beam tracing approach to acoustic modeling for interactive virtual environments', in *Proceedings of the 25th annual conference on Computer graphics and interactive techniques - SIGGRAPH '98. the 25th annual conference*, Not Known: ACM Press, pp. 21–32. doi:10.1145/280814.280818.

Gerzon, michael a. (1975) 'Recording concert hall acoustics for posterity', *journal of the audio engineering society*, 23(7), pp. 569, 571.

Gerzon, M.A. (1973) 'Periphony: With-Height Sound Reproduction', *Journal of the Audio Engineering Society*, 21(1), pp. 2–10.

Greek - Roman Theatre Glossary (Ancient Theatre Archive Project) (no date). Available at: <https://www.whitman.edu/theatre/theatretour/glossary/glossary.htm> (Accessed: 21 November 2021).

Hines (2019) *Tyndaris, Tindari Theatre Commentary*, *Whitman.edu*. Available at: <https://www.whitman.edu/theatre/theatretour/Tyndaris/commentary/Tyndaris.commentary.htm> (Accessed: 6 December 2021).

ISO 3382-1:2009 'Measurement of room acoustic parameters - part 1: performance spaces.' (2009) ISO. Available at: <https://www.iso.org/cms/render/live/en/sites/isoorg/contents/data/standard/04/09/40979.html> (Accessed: 5 December 2021).

Katz, B., Murphy, D. and Farina, A. (2020) 'The Past Has Ears (PHE): XR Explorations of Acoustic Spaces as Cultural Heritage', in, pp. 91–98. doi:10.1007/978-3-030-58468-9_7.

Kimmelman, M. (2015) 'Dear Architects: Sound Matters', *The New York Times*, 29 December. Available at:

<https://www.nytimes.com/interactive/2015/12/29/arts/design/sound-architecture.html>.

Kronlachner, M. (2014) 'Plug-in Suite for Mastering the Production and Playback in Surround Sound and Ambisonics', in.

Kronlachner, M. and Zotter, F. (2014) 'Spatial transformations for the enhancement of Ambisonic recordings', in.

Lecture sulla meccanica delle Murature Storiche (no date). Available at: <http://www.aracneeditrice.it/aracneweb/index.php/pubblicazione.html?item=9788865142301> (Accessed: 15 November 2021).

Lisa, M., Rindel, J. and Christensen, C. (2004) 'PREDICTING THE ACOUSTICS OF ANCIENT OPEN-AIR THEATRES: THE IMPORTANCE OF CALCULATION METHODS AND GEOMETRICAL DETAILS', in.

Murphy, D.T. (2006) 'ARCHAEOLOGICAL ACOUSTIC SPACE MEASUREMENT FOR CONVOLUTION REVERBERATION AND AURALIZATION APPLICATIONS', in.

Nachbar, C. *et al.* (2011) 'AMBIX -A SUGGESTED AMBISONICS FORMAT'.

Narbutt, M. *et al.* (2020) 'AMBIQUAL: Towards a Quality Metric for Headphone Rendered Compressed Ambisonic Spatial Audio', *Applied Sciences*, 10, p. 3188. doi:10.3390/app10093188.

Noisternig, M. (2018) 'EMPAC Spatial Audio Summer Seminar 2018', in. *EMPAC Spatial Audio Summer Seminar 2018*.

Parco Archeologico di Tindari (2020) 'Relazione tecnica, Lavori Di Adeguamento Del Teatro Greco Di Tindari e Valorizzazione Integrata Dell'area Archeologica'.

Rindel, J.H. (2013) 'Roman Theatres and Revival of Their Acoustics in the ERATO Project', *Acta Acustica united with Acustica*, 99(1), pp. 21–29. doi:10.3813/AAA.918584.

'The importance of sound in today's world: promoting best practices. Tech. Rep. Resolution 39 C/49, UNESCO' (2017). Available at: <https://unesdoc.unesco.org/ark:/48223/pf0000259172>.

'The Past Has Hears (PHE) JPICH Conservation and Protection Call Application' (2020).

UNESCO - Text of the Convention for the Safeguarding of the Intangible Cultural Heritage (2018). Available at: <https://ich.unesco.org/en/convention> (Accessed: 21 November 2021).

‘Wikipedia’ (2021) *Wikipedia*. Available at: https://en.wikipedia.org/w/index.php?title=Just-noticeable_difference&oldid=1055706080 (Accessed: 5 December 2021).

Zotter, F. and Frank, M. (2019) *Ambisonics: A Practical 3D Audio Theory for Recording, Studio Production, Sound Reinforcement, and Virtual Reality*. doi:10.1007/978-3-030-17207-7.

LIST OF FIGURES

Figure 1: Native 2D first-order Ambisonic recording with an omnidirectional and a figure-of-eight (Zotter and Frank, 2019)	9
Figure 2: Spherical Harmonics in cartesian 3d space (Farina, 2017).....	10
Figure 3: Comparison between spherical harmonics representations. (Spherical Harmonic Basis Functions, 2021) Graphical elaboration by the author.....	10
Figure 4: The ordering of ACN (to the left) and the ordering of FuMa (to the right).....	12
Figure 5: Study on sound propagation, reflections obtained with a plan wall (a), with an alveolar wall (b), and with the reproduction of the ancient theatre of Orange scaenae frons (c). Images from (Canac, 1967).....	14
Figure 6: General Plan in scale 1:5000, courtesy of Parco Archeologico di Tindari (2020). Graphical elaboration by the author	20
Figure 7: Photo of the current state of the theatre of Tindari, taken during the measurement campaign of 2015 (curtesy of DENERG).....	22
Figure 8: General Plan of the theatre after the restauration works of 1965 (Bernabò Brea, 1965).	23
Figure 9: Longitudinal section of the theatre after the restauration of 1965 (above) and reconstructive section of the Hellenistic configuration (Bernabò Brea, 1965).....	24
Figure 10: Measurement set-up: S1 and S2 indicate the source positions. R1—R9 indicate the receiver positions. O is the centre of the orchestra (at a distance of 1 m from S1, to the left, on the same horizontal axis) and β is the angle from the scenery line and the direction that joins the source and the receiver (Astolfi et al., 2020).....	25
Figure 11: Sketchup view with the materials assigned by G. Benvenuto for her calibration model (Benvenuto, 2020).....	28
Figure 12: (next page) Reconstruction of the historical phases of the theatre (Benvenuto, 2020).....	32
Figure 13: Categorization of the acoustic modelling methos by M.Vorländer. The more recent Finite-difference time-domain method (FDTD) is missing from the list. (Vorländer, 2020).....	36
Figure 14: Representation of the contributions of ISM, ESM and RRM to the generation of the IR. Relation between Energy and Transition Order. (Christensen, Koutsouris and Gil, 2020).....	37
Figure 15: Representation of the contributions of ISM, ESM and RRM to the generation of the IR. Relation between Sound Pressure Level and Time. (Christensen, Koutsouris and Gil, 2020).....	37
Figure 16: Comparison between beam tracing methods: Cone Traing (left) and Pyramid Tracing (right).....	38

Figure 17: comparison of a detail of the old model (in yellow overlay) and the new one (in gray).....	40
Figure 18: Axonometric view of the model in Autocad showing the the scattering coefficient at 707Hz for every surface of the calibration	43
Figure 19: Room settings in Odeon.....	44
Figure 20: settings for Ramsete Tracer	44
Figure 21: Reconstruction of the Plan of in the Hellenistic period (Bernabò Brea, L. 1964-1965).....	48
Figure 22: Graphic reconstruction of the scaenae frons (Bernabò Brea, L. 1964-1965).....	49
Figure 23: Axonometric view of models used for the Hellenistic simulation (above) and for the original Greek configuration. The properties of the materials illustrated are the used for the same material in the calibration model.	50
Figure 24: Hypothetical structural solution for the designing of the shell. Image courtesy of Giovanni Bouvet	55
Figure 25: A ssonometric view in Ramsete.....	56
Figure 26: an example of disturbing late reflection traced in Ramsete.....	59
Figure 27: Render of the 3d recontruction of the Hellenistic configuration	66
Figure 28: Render of the 3d of the current state with the addition of the reflective acoustic shell designed by G.Bouvet.....	65
Figure 29: Render of the 3d of the current state with the addition of the reflective acoustic shell designed by G.Bouvet.....	64

LIST OF TABLES

Table 1: Acoustic qualities and corresponding subjective listeners aspects (Bo, 2017).....	18
Table 2: Basic information about the theatre of Tindari	19
Table 3: Coordinates of the Receiver in the calibration model of Giulia Benvenuto. Graphical elaboration by the author.....	27
Table 4: absorption and scattering coefficient of materials assigned by G. Benvenuto for her calibration model (Benvenuto, 2020).....	29
Table 5: diagram of the absorption coefficient of materials assigned by G. Benvenuto for her calibration model (Benvenuto, 2020).....	29
Table 6: Percentage of the measured IRs exceeding a certain decay range of INR (E.Bo, 2017)	30
Table 7: : Validation of the T20 of the calibration model of 2020 with the MAD method (Benvenuto, 2020)	31
Table 8: : Validation of the G of the calibration model of 2020 with the MAD method (Benvenuto, 2020)	31
Table 9: Results of T20 for the calibration model of Giulia Benvenuto compared to the T20 obtained from the measurement with the dodecaedron.....	31
Table 10: Comparison between the T20 of the different historical configurations per octave band (Benvenuto, 2020).....	34
Table 11: Comparison of Gmid between 500 e 1000 Hz for every receiver for the different historical configurations (Benvenuto, 2020).....	34
Table 12: Comparison between the C50 of the different historical configuration per octave band (Benvenuto, 2020).....	35
Table 13: Comparison between the C80 of the different historical configurations (Benvenuto, 2020).....	35
Table 14: axorbtion coefficients for octave bands used for the calibration.....	42
Table 15: scattering coefficients used for the calibration.....	43
Table 16: T20 acoustical models results compared with the results of the survey	46
Table 17: Confronto tra valori di G medi misurati e simulati per tutti i ricevitori in base alla distanza.....	46
Table 18: C ₅₀ of the calibration model, for all the receivers and sources, expressed as a function of frequency. Standard deviations are reported on the error bars.....	47
Table 19: C ₈₀ of the calibration model, for all the receivers and sources, expressed as a function of frequency. Standard deviations are reported on the error bars.....	47
Table 20: T20 of the Hellenistic acoustical models compared to the results of the survey of 2015.....	51

Table 21:: C_{mid} of the Hellenistic acoustical model for every receiver compared to the results of the survey of 2015.....	51
Table 22: C_{50} of the Hellenistic acoustical model, for all the receivers and sources, expressed as a function of frequency. Standard deviations are reported on the error bars.	52
Table 23: C_{50} of the Hellenistic acoustical model, for all the receivers and sources, expressed as a function of frequency. Standard deviations are reported on the error bars.	52
Table 24: T20 of the Greek acoustical models compared to the results of the survey of 2015.....	53
Table 25: C_{mid} of the Greek acoustical model for every receiver compared to the results of the survey of 2015.....	53
Table 26: C_{50} of the Greek acoustical model, for all the receivers and sources, expressed as a function of frequency. Standard deviations are reported on the error bars.....	54
Table 27: C_{50} of the Greek acoustical model, for all the receivers and sources, expressed as a function of frequency. Standard deviations are reported on the error bars.....	54
Table 28: T20 of the current state optimized with the reflective Shell.....	57
Table 29: C_{mid} of the current state optimized with the reflective Shell.	57
Table 30: C_{50} of the current state optimized with the reflective Shell, for all the receivers and sources, expressed as a function of frequency. Standard deviations are reported on the error bars.	58
Table 31: C_{80} of the current state optimized with the reflective Shell, for all the receivers and sources, expressed as a function of frequency. Standard deviations are reported on the error bars..	58